جامعة أبو بكر بلقايد
UNIVERSITÉ DE TLEMCEN

Pan African University
Institute of Water and Energy Sciences

Institute of Water and Energy Sciences (Including Climate Change)

Evaluation and Analysis of crystalline PV modules performance characteristics degradation in a sub-Saharan environment after ten years of exposure: Case study of Senegalese environment.

SALIF SOW

Date: 05/09/2017

*Master in **Energy, Engineering track***

President: Dr. Souhila Bensmaine

Supervisor: Prof. Cheikh Mohamed Fadel KEBE

Co-supervisor: Dr. Ababacar NDIAYE

External Examiner: Dr. Francis Kemausuor

Internal Examiner: Dr. Abdellah Benyoucef

Academic Year: 2016-2017

DEDICATION

To my dear parents Serigne Khassim SOW and Kadiata Yoro Sow

To my kind, beloved and devout wife Alima SOW

To my dear brothers,sisters, half-brothers and sisters, Aliou, Faty, Aissata, Mbaré, Baty, Penda, Fallou, Yoro Abdou , and Babacar

To my aunts Amy Gadiaga, Adama Ndiaye, Penda, Mairam Tiga and Ndeye Ndiaye

To my late parents Yoro Sow, Penda Sow and Moussou

To My Grandparents Yoro and Tiga SOW

To my dear nephews and Salif, Papa Wagne and Yacine Sow

In Memory of my dear brothers Cheikh Ahmed KA and Alhassan BA

To my family in law (Kalidou SOW, Ngoné KA, Ndeye Amath, Aicha, Aby, SEykou, Lam , Amadou)

To my friends Ababacar KA, Abdou Lo Niang, Mbaye Lo, Ousmane Sy, Oumar Diallo, Yahya Ngom, Khadim Ndao, Amadou Fall and Mouhamed Sall

ACKNOWLEDGMENTS

First, I would like to express my deepest gratitude to Prof Cheikh Mouhamed Fadel KEBE, who first accepted to work with me and encourage during all the work. He served as an inspiration as I hurdled all of the obstacles involved in the completion of this research work. My upset gratitude to Dr. Ababacar NDIAYE for his interest and valuable suggestions to improve this work.

Moreover, I would like to thank all the members of the "Centre International de Formation et de Recherche en Energie Solaire (CIFRES)" leaded by the excellent Prof. Papa Alioune NDIAYE. For a first university experience in Senegal I really felt at home in this great lab. Special mention to the grand sister and guide Amy MBAYE.

I also wish to extend my appreciation to Dr. Alfred DIENG for his support and accompaniment during the internship at the ASER (Senegalese Rural Electrification Agency). He has been a trainer, a brother, and a director for me. A big thank you to all the ASER team especially to Mr. THIAM (DFER), Mr. Mass Samba DIOP, Mr. Malick NGOM, Mr. Moustapha Cissé NDIAYE, Mr. Yoro BA and all the PGP staff.

I would like to thank my colleagues of the 2nd Cohort Energy Engineering at PAUWES. My sincere gratitude to all those teachers who supervised me during my studies in Tlemcen. Life in this city was made wonderful by all the people around us during those years. Alé THIAM, Ganda TOUNKARA, and my lovely brother BACHIR (Moudj) Thank you very much for the good times spent together. Cheers to my sport team in Tlemcen particularly to my two masters Dine Ilyass and Rachid Boukhari.

And last but not least, my warmest thanks go my beloved parents. I still remember that first day on my way to the school, But I can't imagine how patient and encouraging you have been during these long years. You are really super human, I cannot thank you enough.

My sincere and profound thanks to my lovely wife Alima SOW who always supported me during this Master thesis. She always managed to Encourage me and dispel my worries and

doubts. She accepted my long absences, and all the sacrifices necessary for the realization of this work. May Allah reward you with the best of rewards.

DECLARATION

I Salif SOW, hereby declare that this thesis represents my personal work, realized to the best of my knowledge. I also declare that all information, material and results from other works presented here, have been fully cited and referenced in accordance with the academic rules and ethics.

Table of Contents

FIGURE INDEX

TABLE INDEX

Abstract. The effects of a sub-Saharan coastal climate on PV modules degradation was studied in this Master thesis. A Mono and a polycrystalline-silicone solar PV module exposed in Dakar, dry and coastal climate, at the extreme West of Senegal was studied. As first inspection in this region, the electrical parameters of two PV modules A and B operated during about 10 years, are measured under standard testing condition(STC) and their I-V characteristics were fitted. The initial I-V characteristics was performed under real conditions and translated to STCs and compared to the measured I-V characteristics at standard test conditions(STC) obtained in PVLAB after exposition. After the operating years, the main important parameters of the studied PV modules: short-circuit current I_{SC}, open circuit voltage $V_{OC,}$ maximum power P_{MPP}, nominal current I_{MPP} and Voltage V_{MPP} are evaluated and then compared to the initial parameters obtained during initial exposition to estimate their degradation.

Moreover, the defects that affected the PV module are explored by visual inspection, Electroluminescence (EL) and thermography (IR) imaging methods. The results show absolute degradation of maximum power (ΔP_{MPP}) nearing -5.35 % and -2.92% for the mono and polycrystalline silicon operating about 10 years. The inspection reveals many degradations in both modules. Most of the degradations due to the climate are found in the mono and a very advanced I_{SC} mismatch is found with the IR image. The polycrystalline has many mechanical defects that's does not too much affect the performance characteristics.

Key words: solar, photovoltaic, degradation, performance, electroluminescence imaging, thermography imaging.

Résumé. Les effets d'un climat côtier subsaharien sur la dégradation des modules solaire photovoltaïques ont été étudiés dans cette thèse de Master. Deux module photovoltaïques un mono et un polycristallin-silicone exposé à Dakar, climat sec et côtier, à l'extrême ouest du Sénégal ont été étudié. En première inspection dans cette région, les paramètres électriques des deux modules photovoltaïques A et B qui ont fonctionnés pendant environ 10 ans sont mesurés dans des conditions d'essai standard (STC) et leurs caractéristiques I-V ont été tracés. Les caractéristiques I-V initiales avaient été mesurés dans des conditions réelles et traduites en STC et comparées aux caractéristiques I-V mesurées aux conditions d'essai standard (STC) obtenues au PVLAB après exposition. Après les années d'exploitation, les principaux paramètres des modules photovoltaïques étudiés : courant de court-circuit I_{SC}, tension de circuit ouvert V_{OC}, puissance maximale P_{MPP}, courant et tension nominal I_{MPP} et V_{MPP} sont évalués puis comparés aux paramètres initiaux obtenus lors de l'exposition initiale permettant d'estimer leurs dégradations.

En outre, les défauts qui ont affecté le module PV sont explorés par des méthodes d'inspection visuelle, d'électroluminescence (EL) et de thermographie (IR). Les résultats montrent une dégradation absolue de la puissance maximale (ΔP_{MPP}) proche de -5.35% et -2.92% respectivement pour le panneau mono et polycristallin qui ont fonctionnés pendant environ 10 ans. L'inspection révèle de nombreuses dégradations sur les deux modules solaires. La plupart des dégradations dues au climat sont retrouvées sur le monocristallin et une disparité très avancée de production des cellules est révélée par l'image IR. Le polycristallin présente de nombreux défauts mécaniques qui n'affectent pas trop les caractéristiques de performance.

Mots-clés : solaire, photovoltaïque, dégradation, performance, imagerie par électroluminescence, imagerie par thermographie.

INTRODUCTION

INTRODUCTION

The use of Renewable Energies becomes more and more necessary for the satisfaction of the world Energy demand, with less negative effects on the environment. Global warming and fossil fuels depletion force the world to seek for solutions to ensure our survival and those of future generations. Africa in particular is facing a critical energy scenario. According to the World Bank, 25 countries in sub-Saharan Africa are in energetic crisis. Only 32% [1] of the population has access to electricity in 2012 with a very high average price of US $ 0.13 [2]per kilowatt hour.

However, the continent can rely on its significant renewable energy resources to improve its situation. Several renewable energy sources are available in different localities. East Africa is known for its large geothermal deposit. The extremities are marked by the presence of remarkable wind potential with an estimated power of 1,300 GW. Hydropower with an available capacity of 238 GW is the most exploited clean energy in the continent. But solar energy remains the most abundant source on the continent. Africa is the sunniest continent of the world. An average radiation of 2650 kWh / m^2 / year, with an estimated sunshine duration of 3500 hours / year could enable the continent to satisfy its energy needs.

Several energy projects based on solar photovoltaic are planned or executed on the continent. Nevertheless, for better exploitation of solar resources, adaptation of technologies to the African environment is essential. The technical characteristics of the existing solar panels are given under the standard testing conditions (STC) corresponding to a mild climate of 25 ° C and a sunshine of 1000W / m^2. These conditions are totally different from the ambient exposure conditions of panels in Africa. In this context, it is pertinent to identify, quantify and compare the major defects or expected modes of failure for the various climates that can be encountered in sub-Saharan Africa (arid, continental, wet or coastal monsoon) and which are very different from the climate of central Europe.

The objective of this Master thesis is to get acquainted with the research on this current topic, which is the degradation of solar panels, with Senegal precisely as an area of

investigation, characterized by a coastal climate. The study will be based on the degradation of the performance of mono and polycrystalline solar panels after about ten (10) years of exposure in a coastal climate precisely at the Polytechnic superior school of Dakar (ESP). The main objective behind this study is to find out the effects of the Senegalese sub-Saharan Coastal climate on Photovoltaic crystalline modules after about ten years of exposer.

Specifically, this involves, two literature review chapters on the state of the art on crystalline PV technologies and the degradation of photovoltaic modules. These two chapters are about stating the crystalline PV technologies and their different performance characteristics. And finally determine the different types of degradation factors.

The second part is about the experimental study. This section is for the presentation of the exposure conditions and the analytical methods used to assess the performance degradation. And lastly the analysis of the data gathered using Electroluminescence (EL) and Infrared Imaging methods. This will finally lead to defects determination with the first and second derivative method.

Chapter I: state of the art of crystalline photovoltaic technologies

Chapter I: STATE OF THE ART OF CRYSTALLINE PHOTOVOLTAIC TECHNOLOGIES

I.1) Introduction

The conversion of solar energy into electrical energy relies on the photoelectric effect, that is to say on the ability of photons to create charge carriers in a material. When illuminating a semiconductor with appropriate wavelength radiation, the energy of the absorbed photons which is greater than that of the energy gap of the material allows electronic transitions from the valence band to the conduction band of the semiconductor, thereby creating Electron-hole pairs, which can contribute to the current conveyance by the material when polarized. This phenomenon called photoconductivity, is the same process used in the Photolytic industry to produce electricity using semiconductors like silicon. Particularly the crystalline form of silicon is the first and most used material for electricity production. This first chapter is a literature review on the state of crystalline photovoltaic cells. It starts with a general description of different crystalline cell technologies. A study on the most important electric characteristics and their evolution will follow. And at the end, we see the importance of the crystalline technology on the photovoltaic market.

I.2) PV Crystalline Technologies

The direct transformation of light into electrical energy always requires a semiconducting material [3]. The semiconductors are used to make cells that when hit by the Solar's light absorb the photons to produce Electricity. They are called photovoltaic solar cells. The first practical solar cell was developed in 1954 at Bell Laboratory [4] , and it was made on crystalline silicone. Solar cells made on crystalline silicon are also called first generation of photovoltaic solar cells. however, PV systems were not considered for terrestrial applications until after the 1973 oil crisis, when the National Science Foundation organized a conference in Cherry Hill, New Jersey, to lay the foundation for a national R&D program in terrestrial PV system [5]. The first practical solar cells were mono crystalline; due to environmental and economical fact, the polycrystalline solar cell was developed lately by

Kyocera. These are the two main technologies mostly used in the world and that will concern our study.

All photovoltaic solar crystalline silicon cells have the same operating principle called the P-N junction. The crystalline silicon is doped by inserting impurities into the semiconductor. To increase the conductivity of the silicon, two different types of materials are added to the silicon to create the N and P layers. To obtain a N-type material, the semiconductor material (generally silicon) is doped with a higher valence element which has more electrons than the semiconductor, such as Phosphorus, in order to add electrons to the conduction band. The conduction is then assured by the displacement of these electrons.

To obtain a p-type material, the semiconductor material is doped with a component with a lower valence, such as Boron, in order to decrease the number of electrons in the valence band. The conduction is then ensured by the displacement of positively charged carriers which are the holes corresponding to the lack of electrons. The fact of having associated two types of materials to create a junction makes it possible to recover the charges before it has recombined into the material which then becomes neutral again. The presence of the P-N junction thus makes it possible to maintain current flow to its terminals [6]. Then, by associating the cells in series and / or in parallels, it gives what is called solar modules. Each module has two external cables attached at the other side of this junction box (**Figure 1**). This allows PV installers to hook the modules up either in series or in parallel and then send the electricity from the solar array downstream towards the main service panel in a home**.**

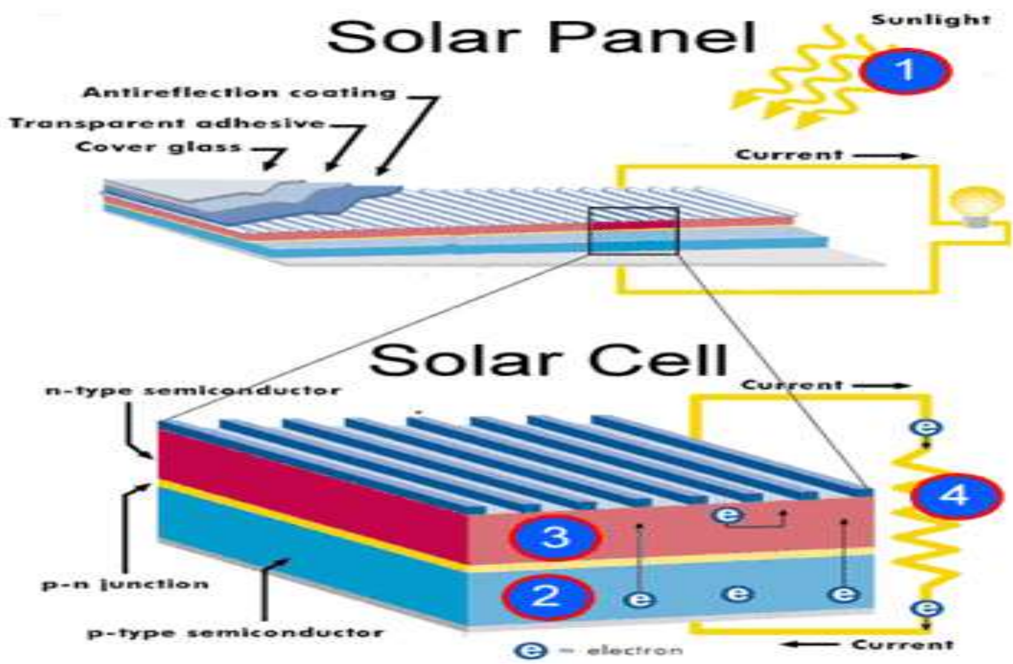

Figure 1:solar photovoltaic principal

I.2.1) Monocrystalline Silicon Solar cells

The monocrystalline (or single-crystal) cells represent the basis technology of photovoltaic energy and It still remains competitive despite its high price compared to the other technologies. Silicon manufacturing can be broken down into four stages: purifying silicon from a metallurgical grade (MG), produced mainly for the steel and aluminum industries, to a much higher purity polysilicon, then forming ingots of silicon of good crystallographic quality from this polysilicon and slicing the ingots into wafers, then processing the wafers into cells and, finally, packaging the cells into a PV module [7]. During the manufacturing, Liquid silicon is intended for the production of monocrystalline silicon mostly by the Czochralski process [8], to ensure a uniform junction during the process, time given and temperature are strictly controlled. And the result of this process is a single and very pure silicon crystal named monocrystalline cell. Its purity gives a uniform blue color (somehow black) (**Figure 2**).

Single-crystal silicon is the most efficient because the crystal is free of grain boundaries, which are defects in the crystal structure caused by variations in the lattice that tend to

decrease the electrical and thermal conductivity of the material [9]. Since the first cells developed with an efficiency of 6%, the silicon monocrystalline does not cease to be increasingly performed. In the last Decade, the average efficiency of commercial monocrystalline silicon modules increased from about 12 % to 20 %. And at the research stage, the record lab cell efficiency is 25.6 % for mono-crystalline [10]. But the method of production is laborious and costly.

Figure 2:Monocrystalline solar cells

I.2.2) Polycrystalline or multi-crystalline Silicon Solar cells

In order to reduce production costs, multi-crystalline silicon, less Expensive than monocrystalline silicon, has been introduced into the industry Photovoltaics since the 70s. Polycrystalline silicon production techniques are much more simple as that of monocrystalline thus far less expensive to implement [11]. Poly-crystalline silicon can be extracted from silicon by heating it up to 1500°C and then cooling it down to 1412°C, which is just above solidification of the material. The cooling is accompanied by origination of an ingot of fibrous-structured poly-crystalline silicon [12]. Whereas monocrystalline solar panels can be identified by their dark blue coloring, polycrystalline solar panels generally have a more blueish tint, and tend to look more scattered or fractured. Multi-crystalline silicon modules have a more disordered atomic structure leading to lower efficiencies, but they are less expensive. Current commercial poly c-Si modules have a higher conversion efficiency of around 13 to 16 %. The record lab cell efficiency is 20.8

% for multi-crystalline silicon wafer-based technology [10]. Their efficiency is expected to increase up to 23 % by 2020 and up to 21 % in the long term [13].

Figure 3:Polycrystalline solar cells

I.3) Electrical characteristics

A solar cell is a typical diode producing electricity. The electron hole created by doping the silicon and the p-n junction technology allow the electrons circulation. At incidence of photon stream onto semiconductor material the electrons are released, if the energy of photons is sufficient. Contact to a solar cell is realized due to metal contacts. If the circuit is closed, meaning an electrical load is connected, then direct current flows. The energy of photons comes in "packages" which are called quants. The energy of each quantum depends on the wavelength of the visible light or electromagnetic waves [14]. Only photons of frequencies corresponding to the possible available energy ΔE for the atom can be absorbed by electron transitions. The relation between frequency and incident photon energy is given by the following equation:

$$\Delta E = h\upsilon = \frac{hc}{\lambda} \quad (1)$$

h is the Planck's constant (6.63 x 10-34 Js)
The frequency υ
and the wavelength λ

I.3.1) Equivalent circuit

The equivalent circuit of a solar cell gives the possibility of modeling the electrical characteristics. It is useful to create a model which is electrically equivalent, and is based on discrete ideal electrical components whose behavior is well defined. An ideal solar cell may be modelled by a current source in parallel with a diode; in practice no solar cell is ideal, so a shunt resistance in paralelle ($\mathbf{R_p}$) and a series resistance($\mathbf{R_s}$) component are added to the model [15].

Considering only the ideal system with out the resistances , solar cell model consists of diode and current source($\mathbf{I_{ph}}$) connected parallelly, the current I the equation**(1)**, using the Shockley equation for an ideal diode representing the PN Junction:

$$I = I_{ph} - I_d = I_{ph} - I_0\{exp[\frac{q(V+IR_s)}{akT} - 1] \quad (2)$$

$\mathbf{I_0}$= reverse saturation current (ampere)

$\boldsymbol{a}$ = diode ideality factor (1 for an ideal diode)

q = elementary charge

k = Boltzmann's constant

T is the temperature of the cell it depends on the ambiant temperature , the NOCT[1](nominal operating cell temperature) and the irradiance H.

$$T = T_a + \frac{(NOCT-20)}{800} H \qquad (3)$$

Real solar cell model with serial and parallel resistance is represented in **Figure 4** , the internal resistances **Rs** and **Rp** resulting in voltage drop and parasitic currents are taken into account. Then the output current is given by the folowing equation:

[1] The nominal operating cell temperature (NOCT) is defined as the temperature reached by open-circuit cells in a module under the following conditions: irradiance on cell surface G = 800 W/m2, air temperature Ta = 20°C, wind velocity = 1 m/s, mounting = open back side.

I = output current (ampere)

I_{ph} = photo generated current (ampere)

I_d = diode current (ampere)

I_p = shunt current (ampere).

$$I = I_{ph} - I_d - I_p \qquad (4)$$

The current in parralel is given by the following expression:

$$I_p = \frac{V+IR_s}{R_p} \qquad (5)$$

Substituting $\mathbf{I_d}$ and $\mathbf{I_p}$ into the third equation produces the characteristic equation of a solar cell, which relates solar cell parameters to the output current and voltage.

$$I = I_{ph} - I_0\{exp\left[\frac{q(V+IR_s)}{akT} - 1\right] - \frac{V+IR_s}{R_p} \qquad (6)$$

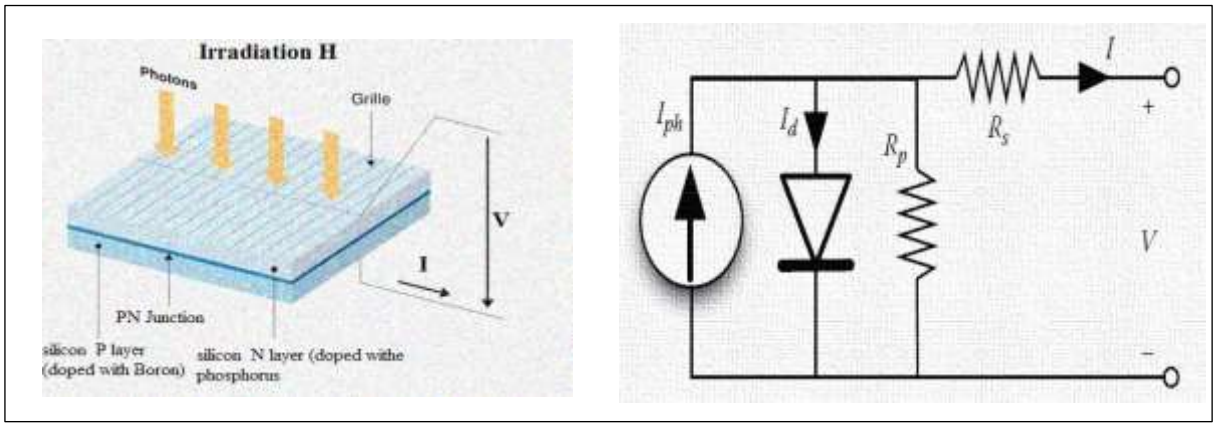

Figure 4: solar cell equivalent circuit

If due to an accident, one cell is broken or simply disconnected from the contiguous ones, then the current of all the cells in series in the string is interrupted and the power contribution of the whole string is missed. To reduce the effect of such events, PV panel manufacturers connect a bypass diode in parallel to short strings of series connected cells, usually two or three depending on the power rating forming the PV panels [16].

I.3.2) The main characteristics

The main parameters that are used to characterize the performance of solar cells are the peak power $\mathbf{P_{MPP}}$, the short circuit current **Isc**, the open circuit voltage $\mathbf{V_{OC}}$, and the fill factor **FF** [17]. The characteristics depend on the type of cells, materials, and technical solutions adopted for manufacturing the cells. These parameters are determined from the illuminated I-V characteristic as illustrated in **Figure 5** The conversion efficiency η can be determined from these parameters.

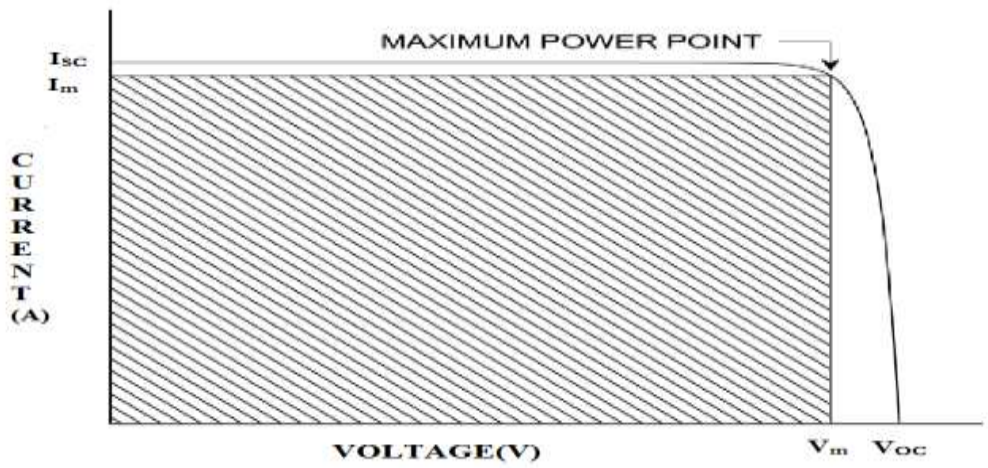

Figure 5: Main characteristics of solar cell under illumination

I.3.2.1) The short circuit current (I_{SC})

The short circuit current **Isc** is the current that flows through the external circuit when the electrodes of the solar cell are short circuited**(V=0)**. The short circuit current of a solar cell depends on the photon flux incident on the solar cell, as shown in **Figure 6** the variation of irradiance also strongly influences the value of the short circuit current. The **Isc** depends on the area of the solar cell. In order to remove the dependence of the solar cell area on **Isc**, the short-circuit current density is often used to describe the maximum current delivered by a solar cell. The maximum current that the solar cell can deliver strongly depends on the optical properties of the solar cell, such as absorption in the absorber layer and reflection. On the contrary, the temperature has a negligible effect on the short-circuit current value. At the same time, very high values of $\mathbf{R_S}$ will also produce a significant reduction in $\mathbf{I_{SC}}$; in these regimes, series resistance dominates and the behavior of the solar cell resembles that of a resistor.

For a high-quality solar cell (low R_S and I_0, and high R_P) the short-circuit current $\mathbf{I_{SC}}$ is approximately equal to $\mathbf{I_{Ph}}$. Crystalline silicon solar cells can deliver under an AM1.5 spectrum a maximum possible current density of **46 mA/cm^2**. In laboratory c-Si solar cells the measured Jsc is above **42 mA/cm^2**, while commercial solar cells have a Jsc exceeding **35 mA/cm2** [17].

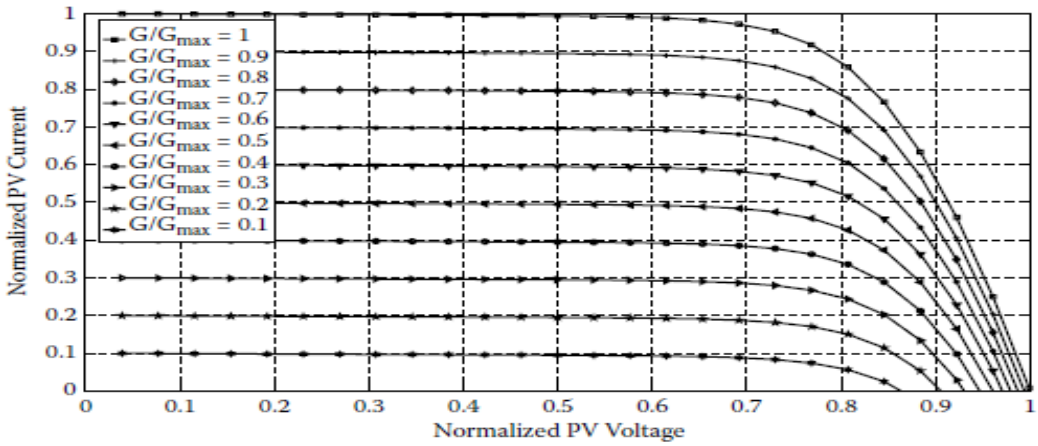

Figure 6:Current vs. voltage characteristic of a PV panel: effect of irradiation H

I.3.2.2) The Open circuit voltage (V_{OC})

The open circuit voltage expressed in millivolts is measured when no current Circulates in the cell **(I=0)**. It depends on the difference between the output of the electrodes and the Shunt resistor. It decreases with temperature (see **Figure 7**) and varies with luminous intensity. The formula bellow extracted from the **equation (5)** by replacing **I=0** gives the Open circuit voltage:

$$V_{OC} = \frac{akT}{q} ln(\frac{I_{ph}}{I_0} + 1) \quad (7)$$

A very low value of $\mathbf{R_P}$ will produce a significant reduction in $\mathbf{V_{OC}}$**, a** badly shunted solar cell will take on operating characteristics similar to those of a resistor. Laboratory crystalline silicon solar cells have a $\mathbf{V_{OC}}$ of up to **720 mV** under the standard **AM1.5** conditions, while commercial solar cells typically have $\mathbf{V_{OC}}$ exceeding **600 mV** [17].

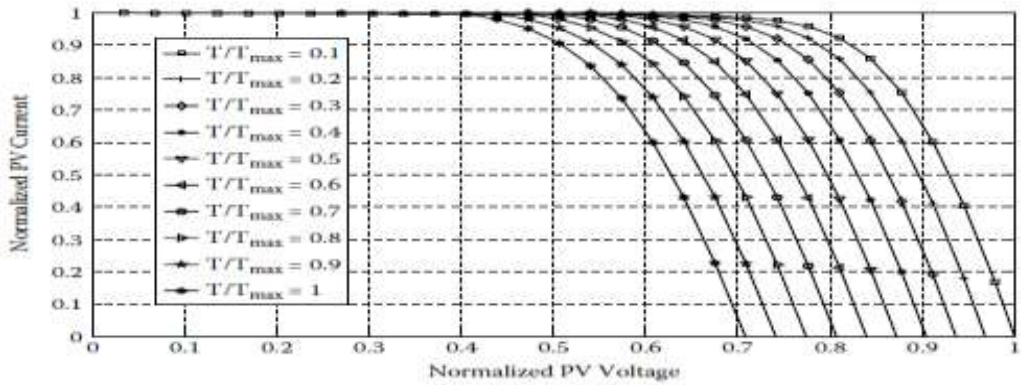

Figure 7:Current vs. voltage characteristic of a PV panel: effect of temperature T.

I.3.2.3) The Maximum Power Point(MPP)

The point of interest of the characteristic curves of a solar PV cell is the Maximum Power Point (MPP). The MPP of a solar cell, is the point on the I-V characteristic of the solar cell, at which the solar cell has the maximal power output. To optimize the operation of PV systems, it is very important, to operate the solar cells (or PV modules) at the MPP. The MPP, at which the current value is I_{MPP}, the voltage value is V_{MPP}, and the power $P_{MPP} = V_{MPP} \times I_{MPP}$ [16] . The **Figure 8** shows that this maximum power is affected by the irradiance and the operating Temperature of the cell. As the irradiance increases and approaches the maximum fixed under the STC the maximum power become higher. In contrast when the temperature increases the maximum power decreases. this is because the increase in temperature increase the resistivity of the cell as described in section (**I.3.1**).

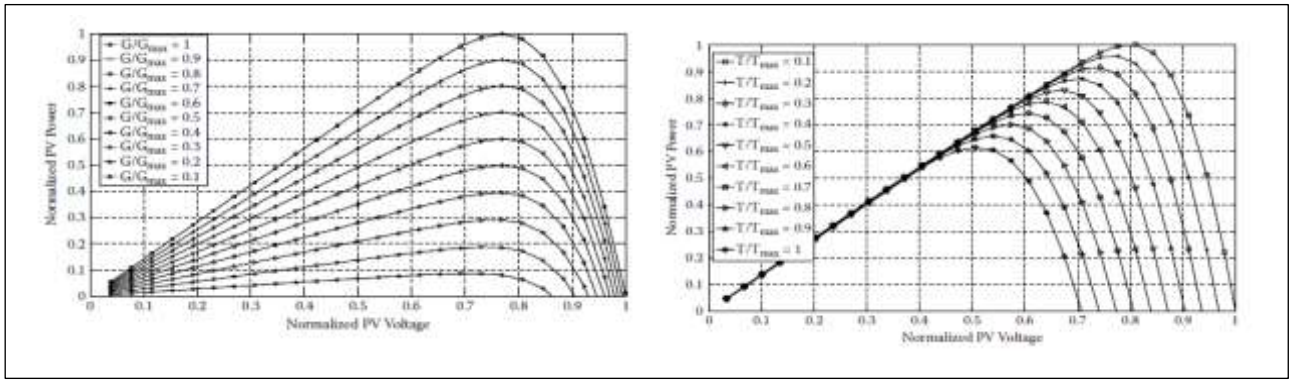

Figure 8:Power vs. voltage characteristic of a PV panel: effect of temperature T and irradiance

I.3.2.4) The Fill Factor (FF)

The short-circuit current and the open-circuit voltage are the maximum current and voltage respectively from a solar cell. However, at both of these operating points, the power from the solar cell is zero. The "fill factor", more commonly known by its abbreviation "FF", is a parameter which, in conjunction with V_{OC} and Isc, determines the maximum power from a solar cell. The FF is defined as the ratio of the maximum power from the solar cell to the product of V_{OC} and Isc. Graphically, the FF is a measure of the "squareness" of the solar cell and is also the area of the largest rectangle which will fit in the IV curve [18] . The following equations gives the FF which depends on the Maximum Power and the

theoretical Power(P_T) corresponding on the case in which the cell can work with its maximum current and voltage:

$$FF = \frac{P_{MPP}}{P_T} = \frac{V_{MPP} \times I_{MPP}}{V_{OC} \times I_{SC}} \qquad (8)$$

P_T: is the output at both the open circuit voltage and short circuit current together

I.3.2.4) The energy conversion efficiency η

The conversion efficiency of a solar cell is defined as the ratio of its electric power output to the incoming light intensity that strikes the cell [19]. The conversion efficiency is determined by measuring the photocurrent (i.e. the electrical current induced by light) as a function of the cell voltage using the formula:

$$\eta = \frac{P_{out}}{P_{in}} = \frac{FF \times I_{SC} \times V_{OC}}{A \times H} \qquad (9)$$

A: is the area of the cell or the module

H: is the irradiance in (W/m^2)

The maximum efficiency (η_{max}) found from a light test is not only an indication of the performance of the device under test, but, like all of the I-V parameters, can also be affected by ambient conditions such as temperature and the intensity and spectrum of the incident light. For this reason, it is recommended to test and compare PV cells using similar lighting and temperature conditions.

I.4) Conclusion

Solar PV is one of the most important renewable Energy source that can participate to the world Energy transition. Since the advent of photovoltaic technology, the crystalline form has carved out the lion's share. Being the first technology developed, it still dominates the market. In 2015 Si-wafer based PV technology accounted for about 93 % of the total production in 2015. The share of multi-crystalline technology is now about 68 % of total production [10]. Africa in particular, has an important solar resource and is developing many projects in the field. However, its conditions are totally different to the STCs. So, it is important to study and know the effect of those condition differences of the solar cell characteristics. The following chapter is about all the factors that can affect the performance of the solar cell and the degradation.

Chapter II: state of the art of PV modules degradation

Chapter II**: STATE OF THE ART OF PV MODULES DEGRADATION**

II.1) Introduction

Solar photovoltaic holds a very important position in the energy transition towards renewable energies. Fraunhofer Institute for Solar Energy(ISE) mentioned that 242 GWp of solar PV were already installed in the world in 2015 [10].According to IRENA Solar PV power generation can grow sevenfold to attend between 1 600 GW and 2 000 GW by 2030 [20]. Africa in particular is expected to install around 90 GW according to Africa 2030 Renewable Energy Roadmap made by IRENA [21]. All this confirms that PV technology is expected to play an important role on the world Energy mix. However, the use of photovoltaic conversion on a large scale is Dependent on certain technical and economic factors linked to the elements of the photovoltaic chain, among others, the photovoltaic panels.

The direct exposition of Photovoltaic generators(Panels) on the environment is a key factor to take into account. As the real outdoor conditions differ from the STC it is expected that the solar characteristics will be affected after a long period of exposure. For this, it is important to understand how the cells are being affected to make accurate predictions of power output decrease over time and return on investment prediction. This chapter is about an investigation on what is already experimented on this field and how the different mode of expected degradation can be determined. Because accurate predictions of return on investment require accurate prediction of decreased power output over time.

II.2) Types and factors of degradation

II.2.1) Degradation types

Degradation is the outcome of a power or performance loss progression dependent on a number of factors such as degradation at the cell, module or even system level [22]. This phenomenon affecting the maximum deliverable power (P_{MMP}), concerns several components of the solar module. These different parts described in **Figure 9** are: **the glass**, **the interconnections between cells**, **the encapsulating material which is generally made of ethylene vinyl acetate (EVA)**, **the protective polymer film which is generally**

made of Tedlar and **the glues that ensure adhesion between the various components of the module** [6]. In all cases, the main extrinsic factors related to performance degradation in field operation include: **temperature**, **humidity**, **precipitation**, **operating voltage**, **dust, snow** and **solar irradiation** [23].

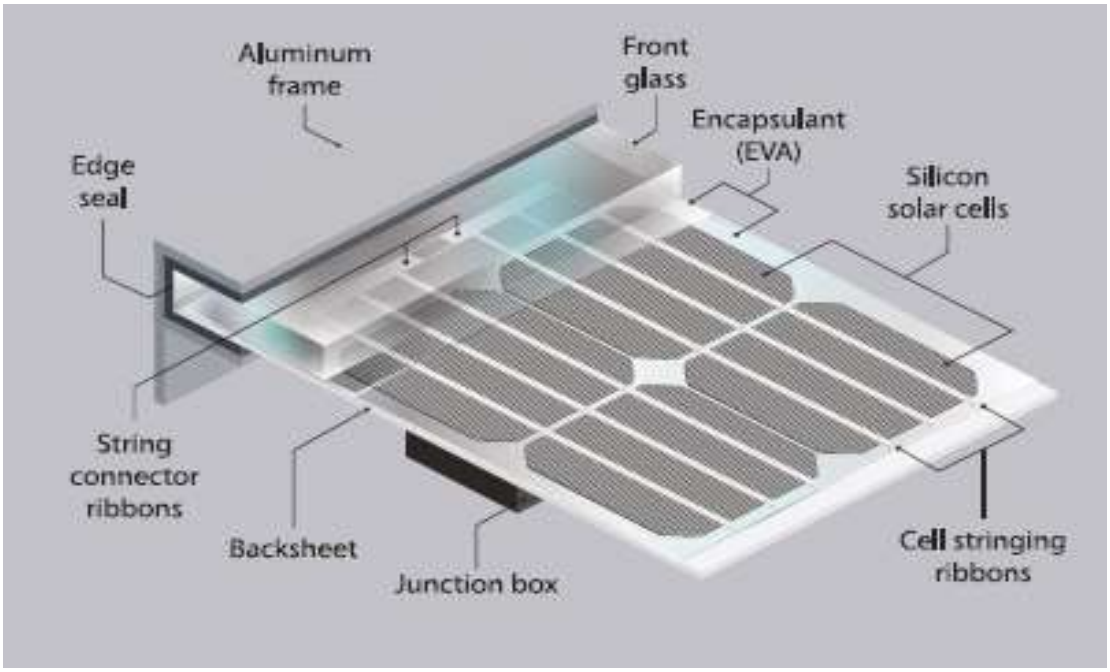

Figure 9:c-Si PV panel components

These various factors mentioned above are at the origin of several degradations types affecting the solar modules performances (see **Figure 10**). The main Degradation phenomena observed in the PV modules operating outdoors for several years include **discoloration** of the EVA, degradation of the anti-reflect (AR) coating, **Potential induced degradation(PID),** degradation of the cell-encapsulat interface(**delamination**). Furthermore, **corrosion** and burn marks were observed mainly on the **busbars and cell interconnections**, usually also visible at the backside of the module together with bubbles, **cracks and tears** of the Tedlar. Finally, **broken cells**, **micro-cracks** and interrupted **gridlines** were also observed [24].

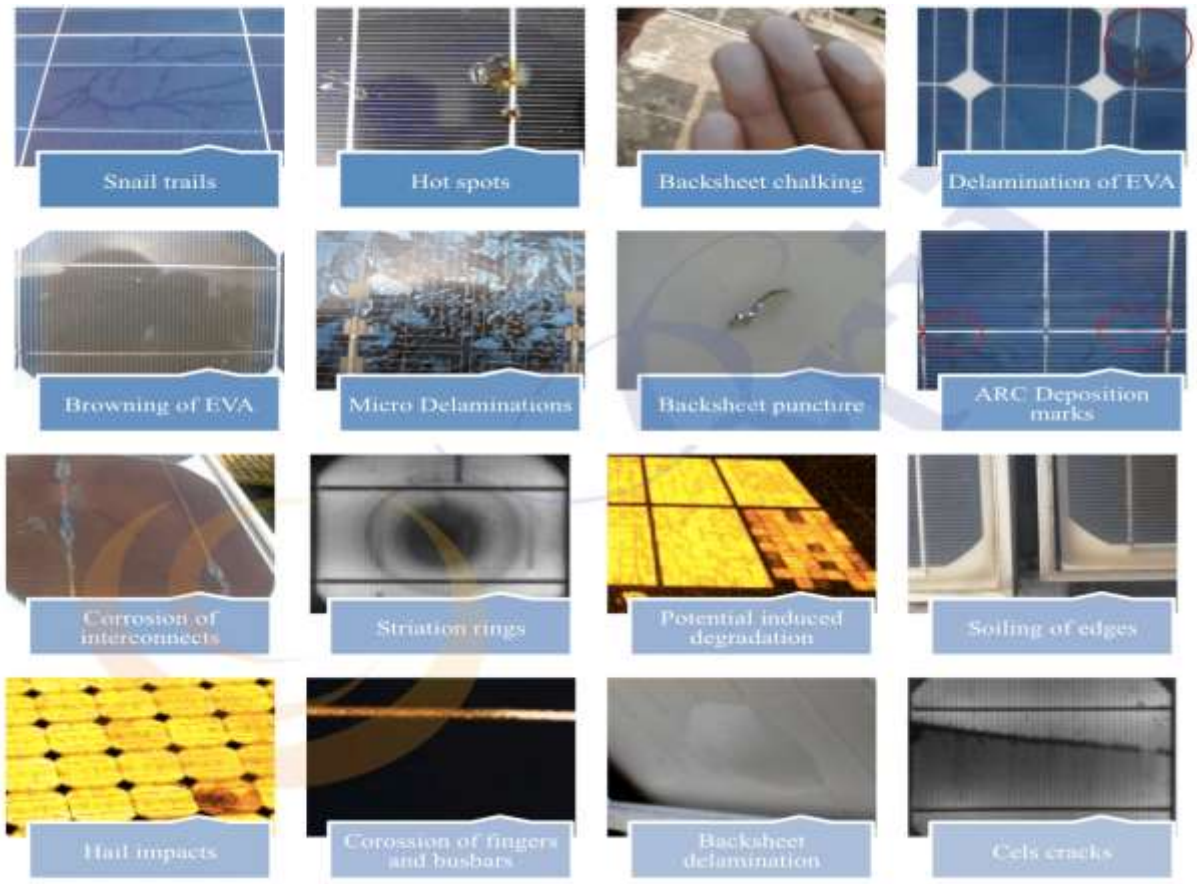

Figure 10: Different Degradation phenomena observed in PV modules operating outdoors

II.2.2) Effects on characteristics parameters

The defects identified above have consequences on the performance characteristic of the modules. The I_{SC} is the most affected characteristic among the others for c-Si modules. Soiling, dust deposit, EVA discoloration and decreased transmission of the short-wavelength photons are the main factors which decrease the I_{sc} of the modules. [25]. According to Hishikawa et al. I_{SC} reduction is due to cloudy discoloration or delamination at cell/EVA interface, increased series resistance R_S, due to the degradation in electrode soldering, or breaking of the cover glass [26]. As shown in **Figure 11** & **12** The FF and the V_{OC} are less affected. Then, the losses in the maximum power is mostly due to losses in the short circuit current. Many degradation rates can be found in the literature depending on the technology investigated and the environment. The National Renewable Energy Laboratory (NREL), in its analytical review on photovoltaic Degradation Rates, has gather

around 2000 degradation rates estimated around the world. This investigation has shown a median value of 0.5% and an average of 0.8% /year [27]. Concerning the other characteristics, The I_{SC} has the highest degradation rate followed by the Fill Factor. For the $V_{OC,}$ yearly degradation rate almost null.

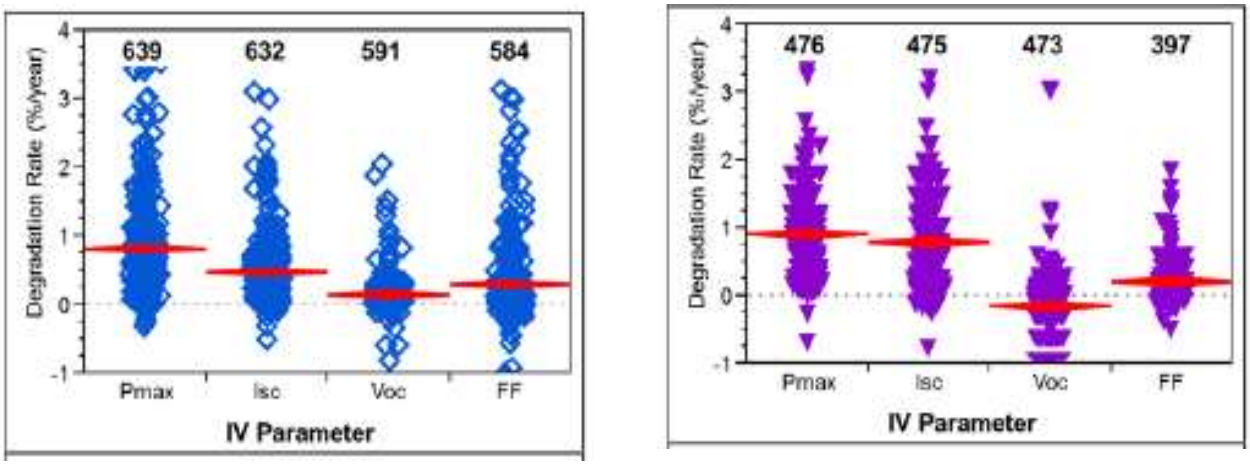

Figure 11:Pmax, Isc, FF and Voc degradation rates for mono-Si (blue) and Poly Si [28]

In the same work done by by D. C. Jordan et al. it is clearly shown that in more than 200 mono and polycrystalline PV modules studied; I_{MPP} also is more affected than V_{MPP}. All this confirms that the Maximum Power degradation is mostly due to Current degradation and a small part to the Fill Factor (FF) [28].

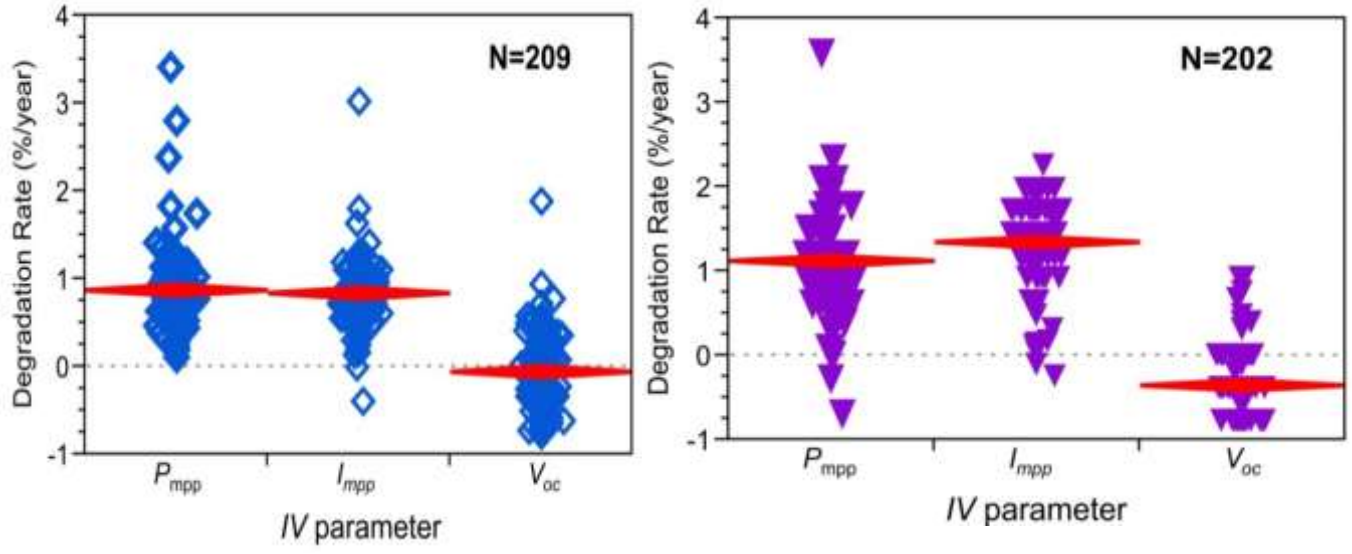

Figure 12:P_{MPP}, I_{MPP}, and V_{MPP} degradation rates for mono-Si (blue) and Poly Si

II.3) PV modules degradation: Diagnostic technics

Failure or degradation diagnostic techniques are used to locate, identify, and evaluate resulting failure or degradation modes. There are different methods that are used to determine or identify failures or defects on solar modules. Several types of existing failures can be located naked eye. This is called the visual inspection of solar PV modules. Bubbles, delamination, Broken cell, cracked cell, discoloration and corrosion can be identified visually [29]. However other methods, or technics may be needed to determine early degradation or non-visual degradation modes. The main diagnostic methods found in the literature are: power Measurement using **IV curve**, **Thermography**, **electroluminescence**, **UV fluorescence**, and **signal transmission method** [29] [6].

II.3.1) Visual inspection

The first step of analysis, allows some defects to be detected by sight. Discoloration, delamination, bubbles, cracks, hot spots often can be detected using this method. This is usually the first step in deciding whether a PV module must be subjected to further tests [30]. The test is performed with the naked eye under a lighting of at least 1000 Lux. Several views are required from different angles to avoid Reflected images and get clear information about the module.

II.3.2) IV Curve Analysis

The IV curve, as described in the previous chapter, presents the variation and relation between the voltage and the current. The solar cell or module is characterized by its short circuit current I_{SC}, the open circuit voltage $V_{OC,}$ the Fill Factor(FF), the Maximum Power ($P_{MPP)}$, the maximum current I_{MPP} and finally the maximum Voltage V_{MPP}. All these parameters discussed in **chapter I** may be affected by different failures types. Virtuani et al. reported that the optical defects influence the Isc, The V_{OC} diminution is due to cell degradation and shunting, and finally the FF is affected by series resistance variation or inhomogeneity in the modules [31]. By quantifying the variation on the characteristics parameters compared to the initial characteristics, it is possible to predict the type of degradation in the module and the maximum power reduction. There are five basic PV

array performance impairments: series losses, shunt losses, mismatch losses, reduced current and reduced voltage (**Figure 13**). Series losses are mainly due to broken internal interconnections, corrosion or poor connection of array wiring causing increase in series resistance.

The shunt resistance increasing caused by cracked or damaged cells, imperfection in cell material and poor edge isolation effect is equivalent to connecting resistors between cell's front and back surfaces the across PV cells. In the other side Mismatch losses (notches or kinks in the IV curve) are often caused by shading, cracked or defective cells, uneven soiling, shorted bypass diode and mismatched cells or modules [32] .

The reduced current is the consequence of uniform soiling, edge soiling, PV module degradation or the weather condition with reduced input irradiance.

Finally, the reduced voltage is the result of the high module temperature, module degradation, shorted bypass diodes. It is relatively insensitive to normal soiling [33].

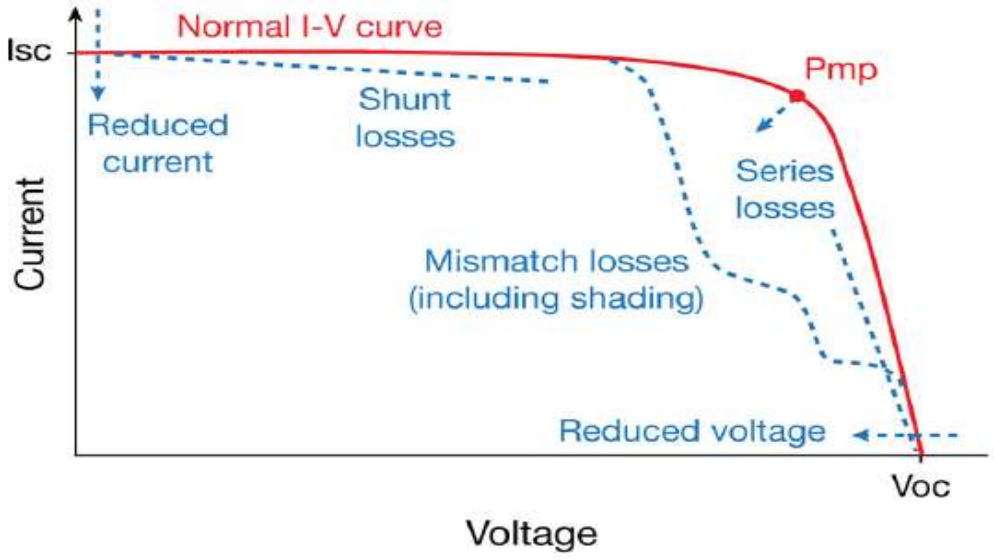

Figure 13: I-V curve signatures for each of the five classes of PV performance impairments: 2 classes affect the height or width of curve. The remaining 3 classes affect the shape of the curve

II.3.3) Electroluminescence Imaging

The Electroluminescence imaging (EL) is a widely-used technique to evaluate the quality of the electrical contacts of solar cells. It consists in applying a direct current to the module and measuring the Photoemission by means of an infrared-sensitive camera. EL imaging

is a useful solar cell and module characterization technique as it is fast, non-destructive and sensitive to the effects of shunt and series resistance and recombination parameters [34]. For electroluminescence investigation, the module is operated as a light emitting diode and the emitted radiation due to recombination effects can be detected with a sensitive Si-CCDs camera. EL is a low light source, that's why a dark environment is necessary in order to make accurate images and avoid the background noise during the measure [35]. The brightness distribution on the photography correlates with the distribution of the open circuit voltage, the minority carrier diffusion length, the series resistance, as well as with the quantum efficiency and the ideality factor of the examined cell [36]. Thus, any electrically inactive parts, within a module or cell, are depicted as dark areas the use of EL for solar cell inspection allows to find **non-uniformities**, **cracks**, **defects, mismatched cell efficiencies**. [37].

II.3.4) Infrared Thermography

The thermography or infrared (IR) imaging is a non-destructive measurement technique, which provides fast, real-time, and two-dimensional distributions of characteristic features of PV modules [29]. Testing of solar cells by infrared (IR) thermography (TG) has been used for a long period and is now a popular and standard testing method. TG IR camera is basically a video camera which captures and saves single images or sequences for different wavelengths in the infrared region [38]. When a mismatch fault occurs in the PV array, a temperature difference between the healthy and an unhealthy module is created, similar to partial shading observed from the terminal [39]. It is specially used for the determination of defects related to temperature. These defects are mostly identified as hot spots. A hot spot heating effect is existent when there is at least one solar cell, within an illuminated module, which presents a short-circuit current abnormally much smaller than the rest of the cells in the module's series string [40]. The measurements with TG can be carried out even with working conditions. IR thermography is a reliable tool for diagnosis of occurring and propagating defects, particularly revealing the existence of hot cells, hotspots on the busbars, and optical degradation in the form of colder bubbles (delamination).

II.3.5) Fluorescence Imaging

Fluorescence(FL) Imaging is a scanning device constructed to allow fluorescence spectroscopic imaging of complete PV modules. This method is can be used to identify cracked cells in the module, EVA degradation, discoloration…. [41] [42]. This method is based on irradiating the modules by UV light and the fluorescence light is measured by a camera. The measurement should be realized in the dark.

In **Table 1**; all the different diagnostic technics are summarized with the different degradation that they can detect.

Table 1: Degradation diagnostic Methods

Methods	Detectable degradation	Controls	Specificities
Visual inspection	Discoloration Delamination Bubbles Cracks burn marks	General appearance of the module	• Test with the naked eye under a lighting of at least 1000 Lux. • Several views are required from different angles. • Reflected images to avoid
IV Curve	Power Currents Tensions Fill factor	Power Currents Tensions Fill factor	• Measures to be implemented in Standard test conditions. • Difficulty controlling standard conditions. Adapted to the module.
Infrared imaging	Hotspot	Images	• CCD camera. Precise and non-destructive technique. • Suitable for cell and module.
thermography	Short circuit Open circuit	Images	• Injection of current. • Suitable for the cell. CCD Detector

Electroluminescence and Photoluminescence Imaging	Cracks	Images	• Injection of current. • Incidental radiation. Dark image
Ultrasonic vibration resonance	Micro cracks	Variation in response frequency	• Ultrasonic excitation of the cell. • Piezoelectric transducer

II.4) Conclusion

The study of PV modules their characteristic parameters degradation is a broad and complex domain. Many degradation modes exist depending on the environment and the technology used. All the PV module components may be affected and differently. At the same time, numerous diagnostic methods are found in the literature. that's why, it is very difficult to define a worldwide degradation rate that can be used for PV projects. It would be very useful to conduct studies for the identification of local degradation modes and the establishment of degradation rates everywhere in the world. The use of these local degradation rates would allow to avoid as far as possible the failure of photovoltaic energy projects.

Chapter III: degradation assessment methodology

Chapter III: DEGRADATION ASSESSMENT METHODOLOGY

III.1) Introduction

Evaluating the degradation of PV modules requires a good knowledge of the environment settings and initial electrical characteristics associated with the modules. As part of this master thesis, a platform is installed on the site of the Ecole Supérieure Polytechnique(ESP) of Cheikh Anta Diop University in Dakar. This locality close to the sea is characterized by a hot and humid climate. The platform is composed of 4 solar modules allowing to ensure lighting and power sockets inside the lab. The calculation and analysis of degradation for this work is focused only on the two modules A and B (**Figure 15**). This chapter first presents the climatic conditions of the site, the experimental measurements and the methods used for PV modules' degradation evaluation. Both crystalline modules (1 mono and poly 1) were investigated to measurement and degradation evaluation with a duration of exposure of approximately 10 years. The degradation of these last is determined in Sahelian environment with the influence of the sea.

III.2) Location and platform test presentation

III.2.1) Presentation of the experimental environment

III.2.1.1) Temperature

The photovoltaic platform shown in figure 17 is used in this study. It is installed at Dakar in Senegal. Dakar is located on the extreme western Africa with geographic coordinates 14.61° North latitude and 17.37° West longitude. In Senegal, the climate is of sub-desert tropical type punctuated by damp summers and dry winters. On the other hand, the DAKAR region, which has an advanced position in the Atlantic Ocean, is characterized by a coastal microclimate. This is strongly influenced by the trade winds and the monsoon coming from the sea. On average, the temperatures are always high. the average daily maximum temperature is 24 ° C from January to March and between 25 and 27 ° C in April, May and December. From June to October, temperatures reach 30 ° C **Figure 14**. [43]

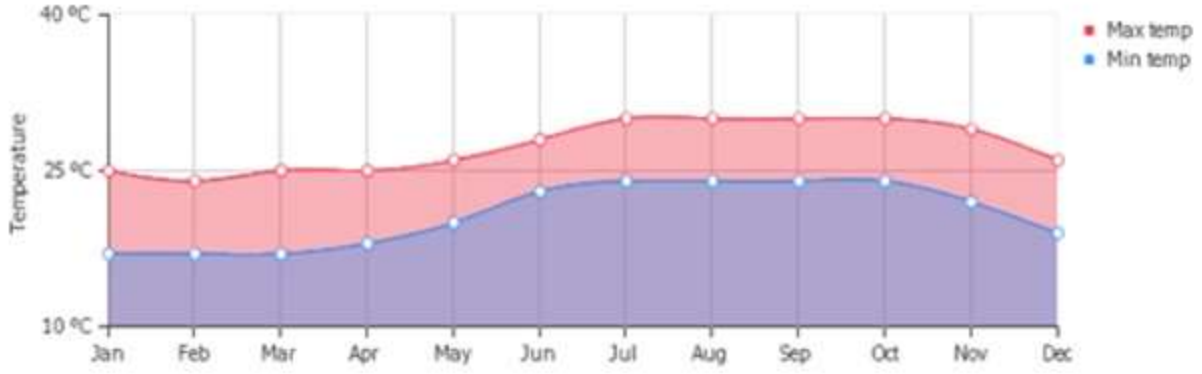

Figure 14: Average min & max temperature in Dakar

III.2.1.2) Radiation and insolation

Radiation and insolation are key parameters, among others, in the quantification of the producible energy but also of the effects of radiation on the photovoltaic material. The radiation is expressed in kWh / m2 while the insolation is expressed in hours. High radiation and insolation values correspond to very high temperatures and low values at low temperatures and vice versa. The average sunshine varies from 7.3h/d during the rainy season when the sky is always cloudy at 9 h / d during the dry season when the sky is clear [44]**.** The highest average monthly value for radiation is 6,92kWh/m^2 /d and is in the period from March to June, while the lowest is 4.57kWh/m^2/d corresponding to the months from July to February (**Table 2**).

III.2.1.3) Humidity

Variations in relative humidity depend in part on the air temperature and the hygrometric characteristics of the air masses. The annual evolution of the relative humidity of the air is also tempered by the maritime influence and the annual average is around 70%. The highest values coincide with the heart of the rainy and low season in the months of April-May and October-December January.

Table 2:Main climatic characteristic of Dakar [45]

Month	Temperature	relative Humidity	Daily solar radiation - horizontal
	°C	%	kWh/m²/d
January	20.7	70.2%	4.89
February	20.7	74.9%	5.80
March	21.0	78.5%	6.57
April	21.4	83.0%	6.92
May	22.8	82.9%	6.71
June	25.6	82.3%	6.21
July	27.1	79.7%	5.60
August	27.4	83.0%	5.34
September	27.6	84.7%	5.34
October	27.6	81.8%	5.53
November	25.8	73.8%	4.98
December	23.4	68.6%	4.57
Annual	**24.3**	**78.6%**	**5.70**

III.3) Platform presentation

The platform used is composed of four (4) modules. Two monocrystalline manufactured by WAAREE in the left. The Two polycrystalline modules in the right are BP Solar products. One module on each technology have been chosen (A & B) to evaluate and analyze the degradation affects about 10 years of operation. The two modules A & B fielded have been installed in same period 2008. The PV modules initial characteristics have been measured using the analyzer IV-400. The obtained IV curve initially designed and the characteristics obtained in exposition location and translated to STC are detailed for each module.

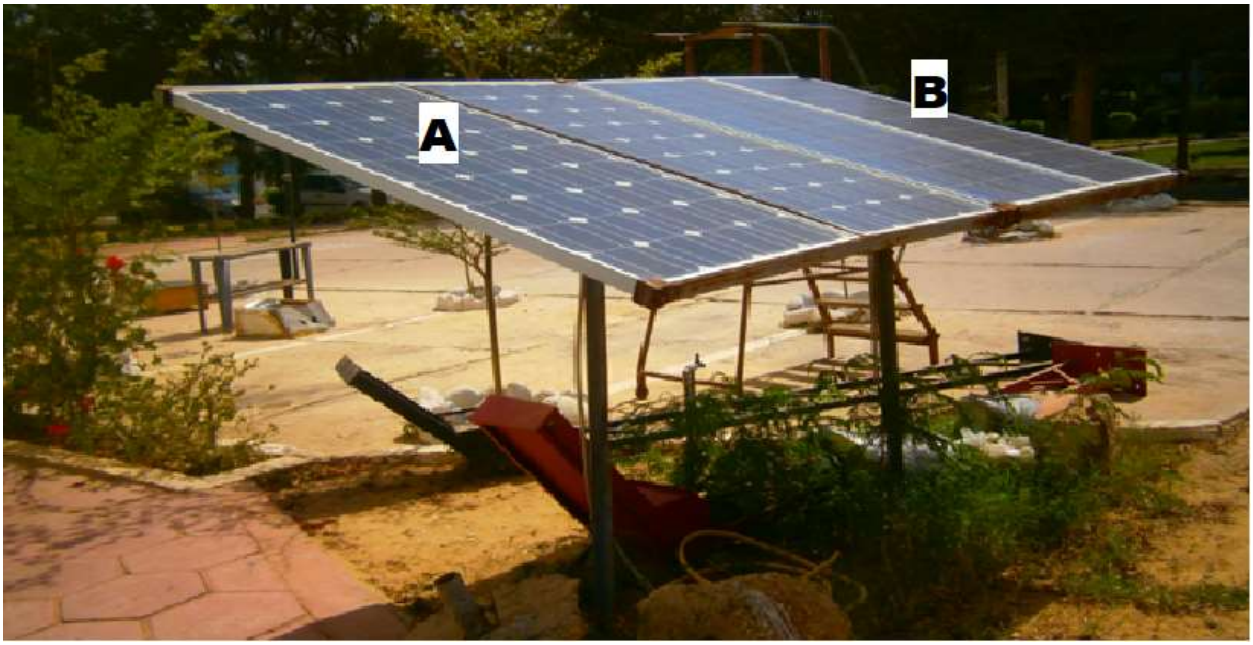

Figure 15: photovoltaic platform installed in Dakar University

III.3.1) Module A & B Electrical characteristics

A monocrystalline solar panel of 106 W_P (given by manufacturer) was used as a reference model for experimentation and simulation. However, the data used for degradation assessment are those measured on-site. The measurement cared out just after the installation of the system on the site, have been done under local conditions and automatically "translated" to the standard testing conditions (STC) (**Table 3**). The main performance characteristics are extracted are gathered in following table. The maximum current and voltage have been used to obtain the P_{MPP}. The maximum power obtained initially is equal to 114W_P.

The second module used (B) is a polycrystalline also of 110 WP according to the data given by the constructor. Like the module A, the initial measurements were established using the IV-400 analyzer. These measurements on site and "translated" to the STCs determine the different performance parameters grouped in Table3. With its 36 polycrystalline cells connected in series, the measured power on site for the poly is equal to 114 WP.

Table 3: Technical characteristics of the PV modules

Module	Module type	Manufacturer	Reference	Characteristics	
Module A	Monocrystalline Silicon	WAAREE	WS-110	Maximum power (P_{MPP})	114 W
				Nominal voltage (V_{MPP})	16.22 V
				Nominal current (I_{MPP})	7.04 A
				Open circuit voltage (Voc)	21.41 V
				Short-circuit current (Isc)	8.56 A
				Fill factor (FF)	62.20%
Module B	Polycrystalline Silicon	BP Solar	WS-110	Maximum power (Pmax)	114 W
				Nominal voltage (Vmax)	17.31 V
				Nominal current (Imax)	6.59 A
				Open circuit voltage (Voc)	21.76 V
				Short-circuit current (Isc)	7.43 A
				Fill factor (FF)	70.50%

III.4) Data acquisition and analysis methodology

III.4.1) Data acquisition

The main objective of this work is to evaluate and analyze the degradation on two crystalline modules exposed for about 10 years. But the main element in all that being to have the effects of the environment on the panel and the consequences generated on the electrical characteristics. For this, the main data used are: the electrical characteristics initially obtained (measurements were carried out by the thesis supervisor) and after the years of exposure, the EL and IR images.

- The initial Electrical performance characteristics are obtained using the analyzer IV-400. Photovoltaic module analyzer I–V 400 carries out the field measurement of the I–V characteristic and of the main characteristic both of a single module and of module strings. The acquired data are then processed to extrapolate the I–V characteristic at standard test conditions (STC). Output current or voltage from the module is measured with the 4-terminal method, which allows extending the measurement cables without requiring any compensation for their resistance, thus always providing accurate measures. Numerical and graphical display of I–V curve is available.

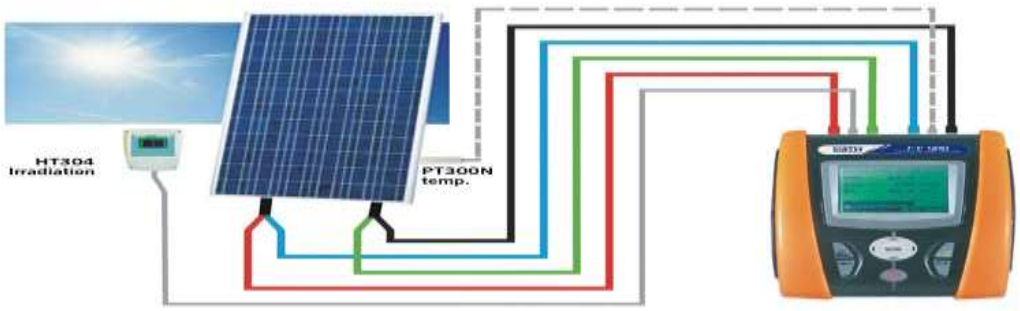

Figure 16: IV-400 Analyzer

- IV curve and electrical characteristics obtained after exposition, have been measured using a lab solar simulator. The PASAN solar simulator is equipped with 4 Xenon flash tubes that generate a pulsed, calibrated and time-steady light. The light travels through a black tunnel and illuminates the module, which is positioned 8 meters away on a uniformly illuminated 3x3 meters surface. Different irradiance levels can be reproduced, however in our case the teste was carried out under STSs. A tracer records the electrical response of the module measuring up to 4000 points of the I-V curve, along with other electrical parameters.

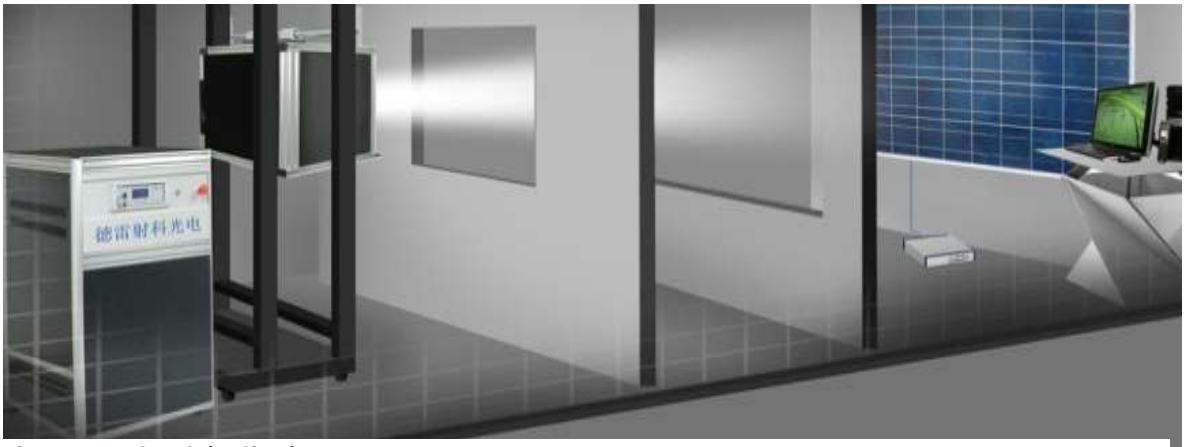

Figure 17: PASAN Solar Simulator

- The set-up for PV EL Imaging is simple, consisting of: shortwave infrared (SWIR) camera with lens darkened enclosure solar cell / module Power Supply. An SWIR camera with In GaAs sensor and a spectral range from 0.9 to 1.7 μm was used in this study for capturing the EL image. Two different EL images have been made using different current. The first with a current equal to I_{SC}, the second was made with just I= 10% I_{SC} wich allows to clearly identify the most affected surfaces.

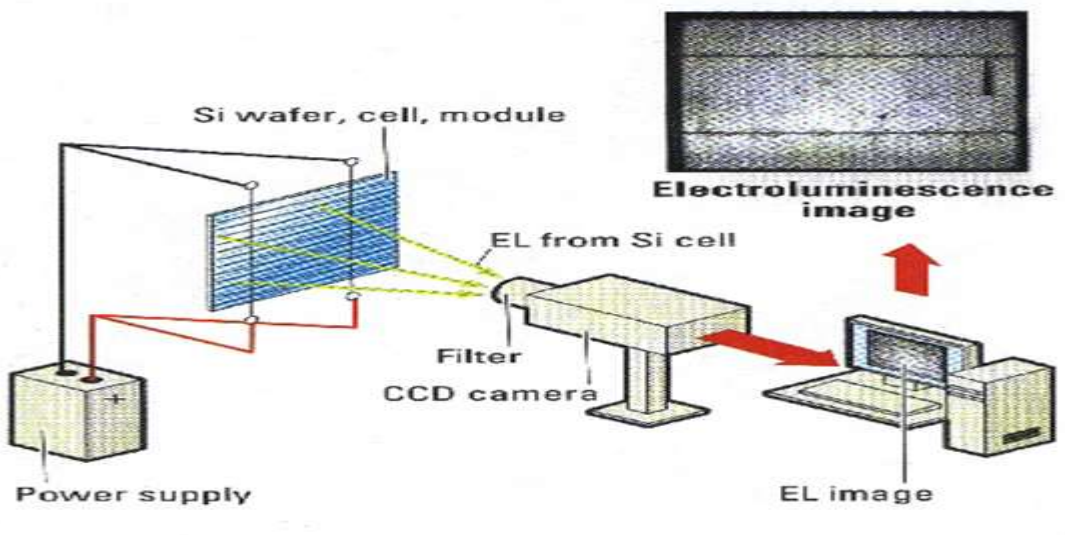

Figure 18: Electroluminescence Imaging

- For IR Imaging, the measuring device is a thermal imaging camera with a surface temperature measurement range of -20˚C to 250˚C and a 31˚ x 22.5˚ field of view, the user can view and save a quick snapshot of temperature patterns in any given area, thus quickly identifying unusual hot or cold spots. With ≤80mK thermal sensitivity, temperature differences of just 0.8˚C are visualized on the 3.5" cooler screen via the 160 x 120-pixel thermal sensor. Three different color palettes give added functionality whilst hot and cold spots can be activated to immediately highlight hot and cold spots in the field of view. A digital read out of the surface temperature at the measurement point is shown alongside both the thermal image and the visible-light picture from the camera.
- The percentage of the surface affected by the different types of degradation is obtained with the GeoGebra software. GeoGebra is a dynamic mathematics software that combines geometry, algebra, spreadsheet, graph, statistics and infinitesimal calculus into a single easy-to-use software. It allows, according to a chosen scale, to quantify the selected surfaces and to put them in color. Thus, these surfaces in comparison with the total surface gives the percentage of the surface affected by the degradation [46].

III.4.2) Analysis approaches

In this study, degradation phenomena observed in PV modules operating in the field for about 10 years are presented. Nondestructive diagnostic techniques including I-V curve analysis, infrared (IR) thermography and electroluminescence (EL) are employed here to assess PV performance and identify the defects. And the software Geogebra with the EL image give important information on the percentage of affected surface. Two Modules that have undergone different stages of degradation, from mechanical and manufacturing defects to severe visual degradation phenomena due to environmental effects, are analyzed, and performance characteristics degradation estimates are given for the 2 different technologies tested, revealing the need for a deeper understanding of PV degradation phenomena that occur under real conditions of operation. The used methods are summarized in **Figure 19.**

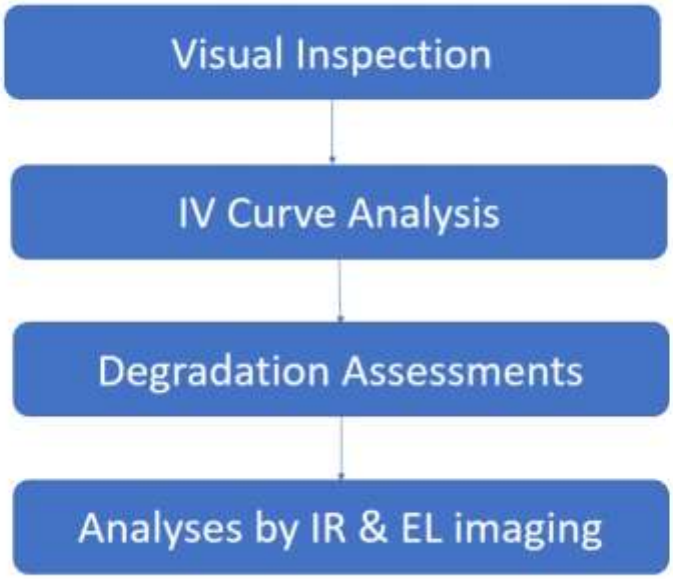

Figure 19: Degradation Diagnostic methodology

III.5) Conclusion

Studying the degradation of photovoltaic modules is not an easy work. Different wherewithal are needed to identify and analyze the degradation of a solar module. Two defects PV technologies operating outdoors about 10 years have been examined and defect detection and diagnosis was carried out through visual inspection, I-V curve analysis, IR thermography and EL imaging. A combination of all these techniques was found important for an in-depth analysis of PV degradation and underlying defects. Visual inspection is the trigger, which leads to more investment to identify almost all defects and quantify the consequences using the other methods cited above. Visual inspection is the trigger. It allows to identify the defects mostly affecting the material. But sometimes this inspection does not give enough information about the necessity of using the other methods. The IV curve allows to predict the defect and to identify the most affected characteristic. EL imaging gave significant insights to the actual physical condition of the modules, and IR thermography shows abnormal behavior due to cells productivity decrease.

Chapter IV: Results and Discussion

Chapter IV**: RESULTS AND DISCUSSIONS**

IV.1) Introduction

In this chapter, the aim is to assess, quantify and analyze the degradation of the two PV modules that operated during nearly ten (10) years in the tropical climate of Dakar located at the extreme west of Senegal. This locality, as described in chapter 3 is marked by a tropical and semi-arid climate. We investigated the degradation of the main important electrical parameters (P_{MPP}, I_{SC}, V_{OC}, I_{MPP}, V_{MPP} and the FF) of two PV modules installed in the University of Dakar.

For further details in addition to the visual inspection, both modules were analyzed by Electroluminescence(EL) and Infrared(IR) imagery. This inspection allows to identify the different defects in the module, quantify the affected surface and analyze the temperature distribution to understand the different performance characteristics degradation that affected the two PV modules.

IV.2) PV MODULE DEGRADATION ASSESSMENT

IV.2.1) Module A: Monocrystalline

IV.2.1.1) Characteristics after 10 years of exposure

After using the module for about 10 years, the performance characteristics were again measured. These measurements obtained at PV LAB in Switzerland are carried out directly in the STC with a simulator. The PASAN tester TC 1.1.3 used, is a pulsed solar simulator, for current-voltage (IV) characterization of photovoltaic modules. The results obtained made it possible to plot the curve IV in blue in **Figure 20**

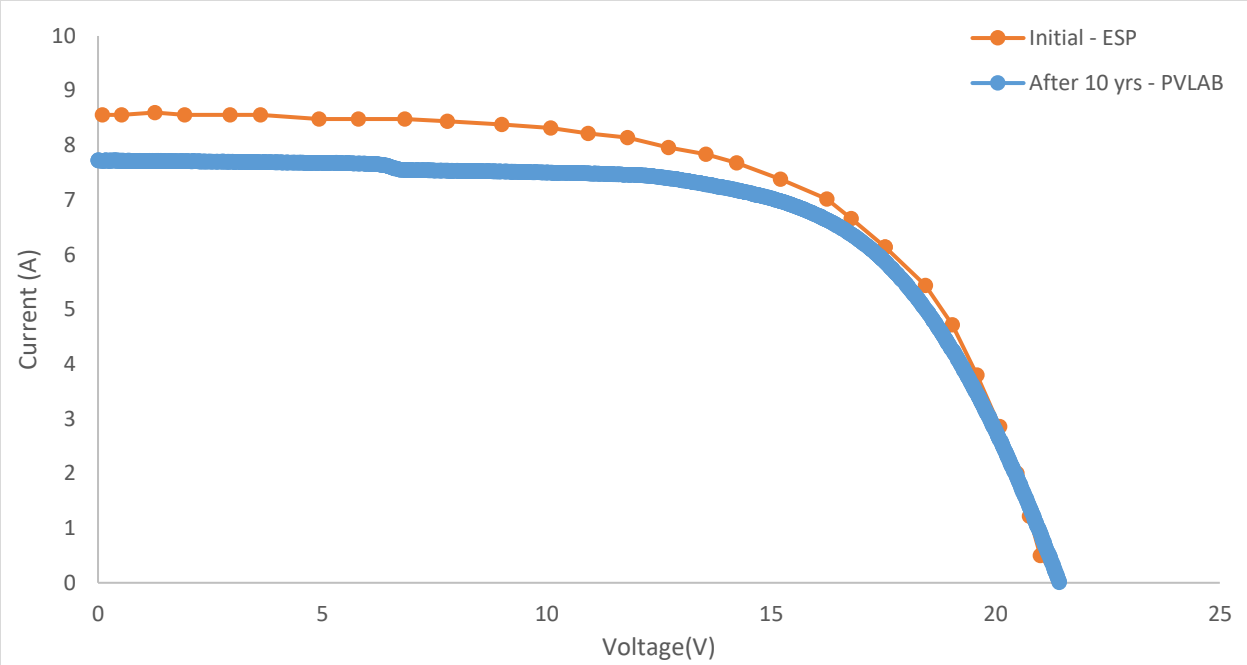

Figure 20:I-V characteristics of PV module A.

The realization of this curve IV in comparison with the initial curve already shows degradation of certain performance characteristics. The short-circuit current I_{SC} from 8.56A to 7.75A is the most affected characteristic. Therefore, the maximum power current I_{MPP} is affected. Initially the maximum power of 114 W obtained with I_{MPP} of 7.02A decreases by 6.095 W. The Nominal current becomes then 6, 67 A.

Table 4: Performance characteristics comparison after about 10 years

Measurements	**P_{MPP} [W]**	**V_{OC} [V]**	**V_{MPP} [V]**	**I_{SC} [A]**	**I_{MPP} [A]**	**FF [%]**
Initial - Measured at ESP	114	21.405	16.24	8.56	7.020	62.2
After 10yrs - Measured at PVLAB	107.905	21.44	16.178	7.750	6.670	**64.9**

IV.2.1.2) Degradation assessment

The measurements initially carried out with the natural sunlight and translated back to the STC with the IV400 analyzer; and those using a simulator in the STC conditions at PV LAB made are used to evaluate the different variations that occurs during the module exposition. The nominal (I_{MPP}) and short circuit (Isc) current, the nominal (V_{MPP}) and the open-circuit (Voc) voltage, and the PV module maximum power (P_{MPP}) degradation are

evaluated by comparing each measured value after 10 years with the reference value obtained with the initial measurements given in **Table 4**. The degradation of these different parameters is expressed in percentage as a function of the difference between the initial normalized values and the obtained after exploitation using the following equations:

$$\Delta I_{SC}(\%) = \frac{\left(I_{SC_{10}} - I_{SC_i}\right)}{I_{SC_i}} \times 100 \qquad (10)$$

$$\Delta V_{OC}(\%) = \frac{\left(V_{OC_{10}} - V_{OC_i}\right)}{V_{OC_i}} \times 100 \qquad (11)$$

$$\Delta I_{MPP}(\%) = \frac{\left(I_{MPP_{10}} - I_{MPP_i}\right)}{I_{MPP_i}} \times 100 \qquad (12)$$

$$\Delta V_{MPP}(\%) = \frac{\left(V_{MPP_{10}} - V_{MPP_i}\right)}{V_{MPP_i}} \times 100 \qquad (13)$$

$$\Delta P_{MPP}(\%) = \frac{\left(P_{MPP_{10}} - P_{MPP_i}\right)}{P_{MPP_i}} \times 100 \qquad (14)$$

The results obtained from the degradation calculations are summarized in **Figure 21**:

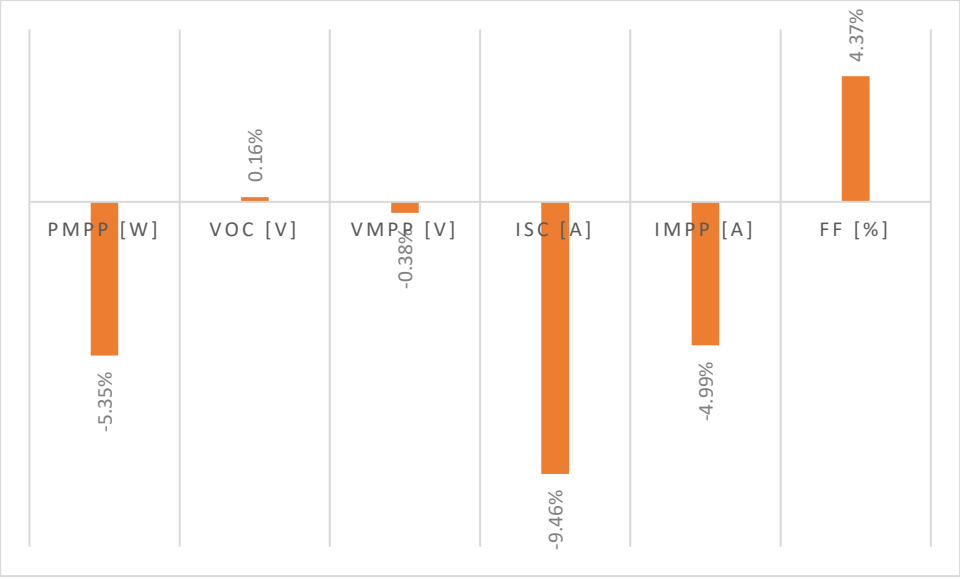

Figure 21:Performance Degradation of module A

From **Figure 21**, it can be seen that the open-circuit voltage is not affected because the calculated degradation is positive. The V_{MPP} also expresses a very slight degradation of just -0.38%. However, the nominal and short circuit current degradation is striking and equal

to -4.99% and -9.46% respectively, which is generally caused by mismatched cells and increase sometimes series resistance increase. Such kind of I-V distribution and I_{sc} reduction refer to irradiation decreases or shaded cells. In general, this is the consequences of operating area reduction or cells properties inhomogeneity. Also, a non-homogeneous temperature distribution could be expected by thermal imaging to confirm the aging of this module. The considerable degradation of I_{MPP} particularly affects the maximum power which is degraded by -5.35%. The fill factor degradation rate is also positive, meaning that the theoretical power degradation ($P_T = I_{SC} * V_{OC}$) is more important than the maximum power diminution.

IV.2.2) Module B: Polycrystalline

IV.2.2.1) Characteristics after 10 years of exposure

After almost 10 years of operation in hot and humid climatic conditions, the PV module I-V curve were measured using pulsed solar simulator the comparison between measurements made initially and after exposition (figure 24) showed that, the short circuit current (Isc) and the open circuit voltage(V_{OC}) did not change too much. However, the trend of the IV curve obtained after the operation years shows a slight decrease in the maximum power. In the literature (**Figure13**), such a change on curve I-V is due to an increase in the series resistance R_S. This variation in resistance mainly affects the PV module operating voltage.

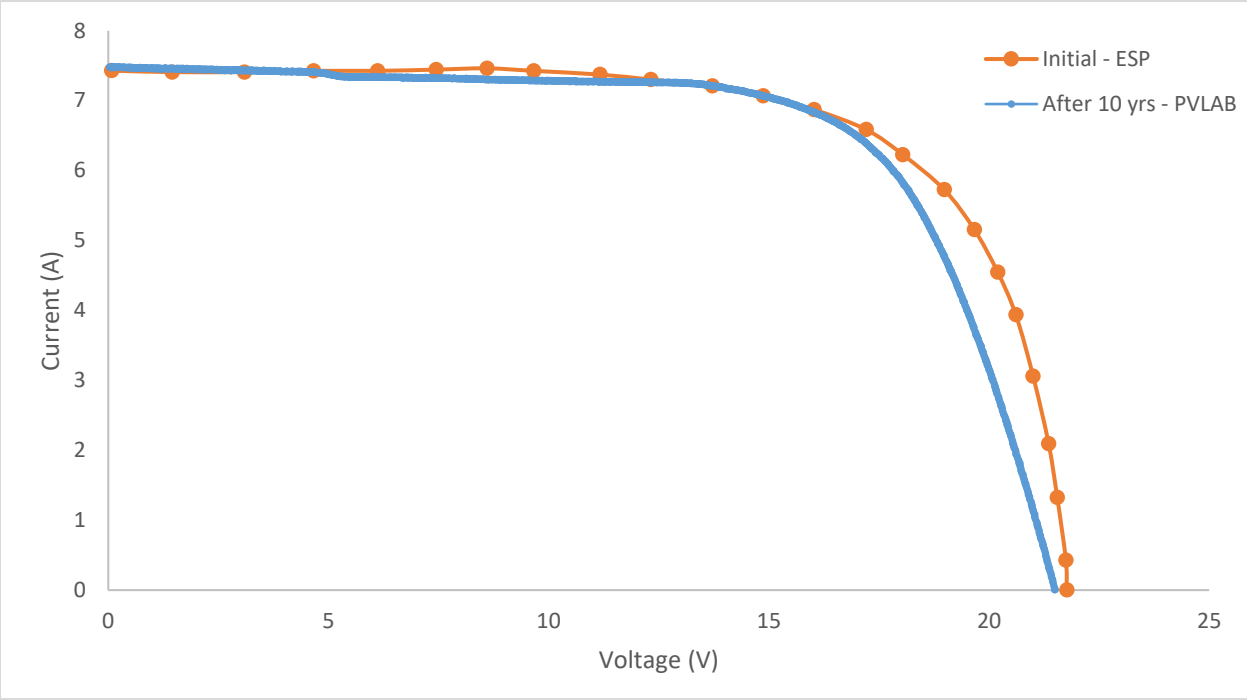

Figure 22: I-V characteristics of PV module B

The comparison between the performance characteristics initially measured and that after the years of operation clearly shows that the nominal(I_{MPP}) and short-circuit (I_{SC}) current have not been affected. However, even if the variation is not too great, among all the parameters, voltage was the only electrical characteristic that deteriorated. The open-circuit voltage goes from 21.765 V to 21.5 V. The nominal voltage(V_{MPP}) has experienced the greatest variation, with an initial value equal to 17.3V, it becomes 16.73V, ie an absolute reduction of 0.6V.

Table 5: Performance characteristics comparison after about 10 years

Measurements	**P_{MPP} [W]**	**Voc [V]**	**Vmpp [V]**	**Isc [A]**	**Impp [A]**	**FF [%]**
Initial - Measured at ESP	114.01	21.765	17.311	7.429	6.586	70.5
After 10 yrs - Measured at PVLAB	110.686	21.502	16.726	7.480	6.618	68.8

IV.2.2.2) Degradation assessment

As for module A, equation from 10 to 14 have been used to evaluate the degradation of performance characteristics. The results obtained are summarized in **Figure 23**. As expected with series resistance increase visible in the I-V curve (**Figure 22**), the maximum power voltage is the most affected characteristic, its absolute deterioration is -3.38%. Indeed, for a PV module exposed for almost 10 years, a degradation of only -2.92% of the maximum power is a good compatibility sign of this technology within the climate. However, it is always necessary to evaluate the different types of defects that affected the module to verify the material defects caused by the tropical climate. The Fill factor (FF) degradation is mainly due to the degradation nominal voltage degradation.

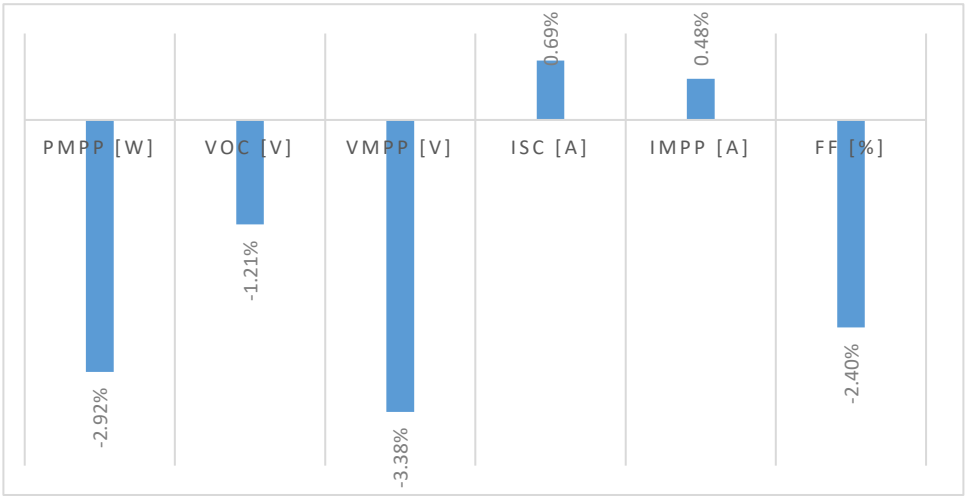

Figure 23: Module B Performance characteristic degradation

IV.2.3) Comparative study

The comparison between calculated degradation of the different characteristics for the two PV modules are summarized in table 6. For the monocrystalline PV module (A), the short circuit current is the most affected characteristic with a degradation equal to -9.46%. The polycrystalline module(B) characteristics are slightly affected, but it is important to mention that the nominal voltage is the most affected parameter. This is to say that the drop in the maximum power output in the two PV modules does not have the same causes. The two modules than have different defects leading to such reduction of the maximum power.

The P_{MPP} degradation is equal to -5.35% for module A, and just -2.92% for module B. thus, electrically the monocrystalline is more affected under such a climate

Table 6: Performance characteristics degradation for the two PV Modules

	P_{MPP} [W]	V_{OC} [V]	V_{MPP} [V]	I_{SC} [A]	I_{MPP} [A]	FF [%]
PV module A	**-5.35%**	**0.16%**	**-0.38%**	**-9.46%**	**-4.99%**	**4.37%**
PV module B	**-2.92%**	**-1.21%**	**-3.38%**	**0.69%**	**0.48%**	**-2.40%**

IV.3) PV DEGRADATION AND DIAGNOSTICS

IV.3.1) Module A: monocrystalline

IV.3.1.1) analysis by electroluminescence (EL)

IV.3.1.1.1) Degradation types identification

Defects in the material of the cell, micro-cracks, broken metallization, shunts, inactive regions are detected via Electroluminescence imaging in **Figure 24**. This El used to identify the defects is made under I_{SC} current. The fault types present in the modules are identified with different colors

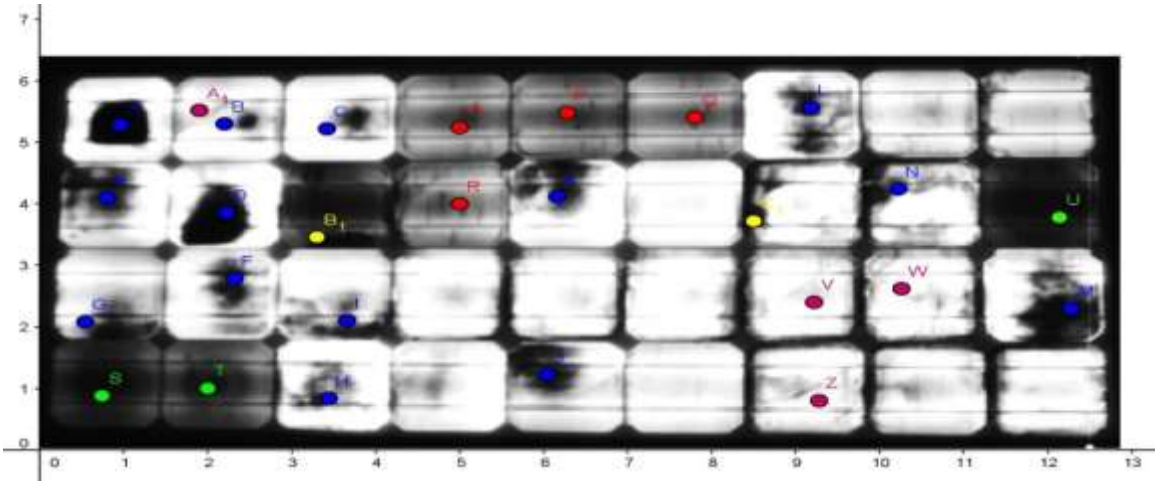

Figure 24: module A EL image with I= Isc

- **Fifteen (15) cells** (blue) have visual impairments such as discoloration and corrosion identified during visual inspection. These types of defects are directly related to climatic conditions mainly humidity.

- **Two (2) cells** with breakages which often occur during transport, packaging or installation of the modules. These types of mechanical damage are caused by insufficient packaging and vibration / shock.
- **Four (4) cells** with casting defects better known by the Contact finger interruptions. These types of defects are usually caused by insufficient screen printing during manufacturing. Because of their significant presence and non-uniform distribution, their remarkable effects on cells productivity are clearly evident.
- **Four (4)** other cells have microcracks, these types of defects such as breaks often occur during transport of the modules. The variation of the intrinsic manufacturing process can also be the cause of cells microcracks. But they are less serious and mostly invisible during visual inspection. However, they may cause deterioration in performance after several years of operation.
- **Three (3) cells** have unspecified dark areas. Several assumptions can be made about the origin of the dark shade: it may come from a local modification of the efficiency favoring non-radiative recombination of the charges, modification of optical proprieties of this zone and therefore the number of photons collected by the detector, or a modification of the contact resistance. These assumptions mean that it is not possible to identify all the types of degradation present in an EL image on the simple visual criterion [35].

In summary, most of the defects identified on the module are due to the effects of the exposure climate conditions. 14 cells suffer from material degradation due mainly to contact of water with the cells. This water often present in moist air causes discoloration and corrosion. Given the climatic conditions of the operating site, it is evident that the high relative humidity of the hot location has effects on the cells. Indeed, Dakar is a very wet place with an annual average of 78.6%.

Table 7: Defects observed in module A

Degradation type	Number of effected cells	Percentage relative to the total number of cell
Micro cracks	**2**	5.56%
Visual degradation	**14**	38.89%
Contact finger interruption	**5**	13.89%
Dark area	**3**	8.33%
breakages	**5**	13.89%

The rest of the defects are for the most part mechanical. Six (6) cells have either microcracks or breaks due to poor handling during transport or laying. Manufacturing defects are fairly present. 4 cells with metallic hits severely affected are identified. 3 other cells have unidentified defects but often come from manufacturing.

IV.3.1.1.2) Affected area Evaluation

The use of the GeoGebra dynamic mathematics software allowed to quantify the total area affected by the different degradation types. The EL image used to determine the surfaces is the one supplied with a current equal to **10% of I_{SC}** (**Figure 25**). An EL image taken at about 10% of the rated current of the photovoltaic module is more suitable for isolated cell parts quantification.

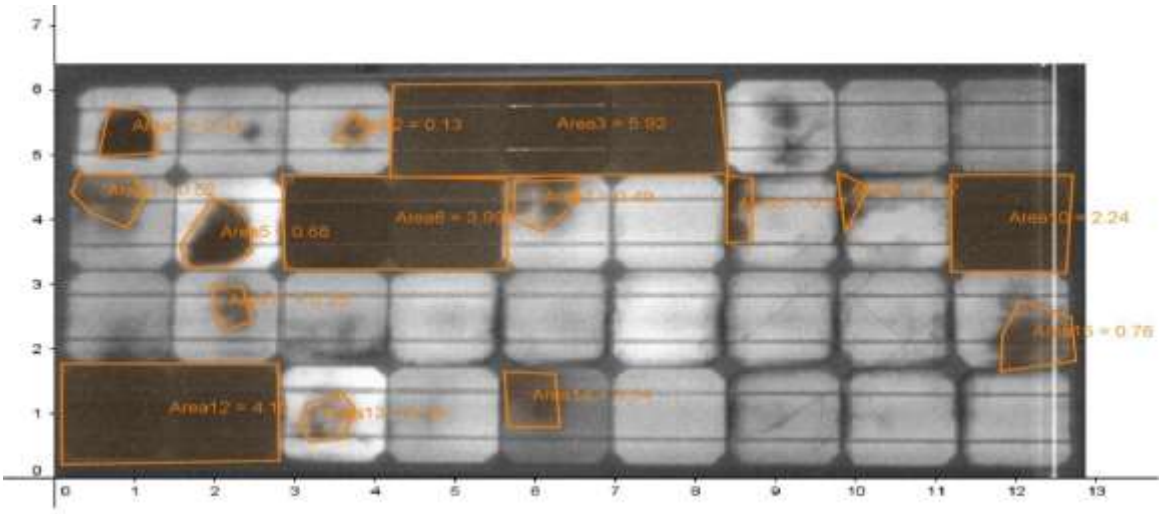

Figure 25: Module A EL image withe I= 10% Isc

The maximum power(P_{MPP}) that the PV module can produce depends strongly on its productive surface as described in Chapter 1. Thus, the evaluation of the affected surface by the different types of degradation makes gives the opportunity to analyze the effects of productive surface decrease on the characteristics.

According to the chosen scale on the **Figure 25**, the panel's total area is 75 cm^2. The fifteen (15) degraded areas evaluation gives a total dark surface of 20.97 cm^2 affected by the different types of defects cited above. Thus, 27.96% of the module's surface has been deteriorated. This materiel degradation of the surface led to a degradation of -5.35% in the maximum power (P_{MPP}). Then, the degradation of 1% of the surface causes a reduction of about 2% in the maximum power. Nevertheless, the black areas should not be interpreted as a totally zero emission, a black zone emits very little compared to the rest of the cell. And this is what causes electrical mismatches and reduce the I_{SC}.

IV.3.1.2)) analysis by infrared imaging (IR)

In a normal PV module, all the cells are considered identical. For a defect less module, the temperature distribution is homogeneous because all the cells have the same characteristics. Thus, PV module thermography image visualization is a very useful tool to state a PV module. Infrared imagery specifically identifies hot spots and cold spots. Hot spots indicate a decline in productivity in these areas, which dissipates the surplus current from other parts as heat. This occurs when the cell is totally or partially shaded, fractured or electrically defective. The severity of this degradation is directly related the cell's temperature. The cold zones highlight the visual degradations. The areas affected by these types of degradation act as insulators. The monocrystalline module IR image in **Figure 26** shows a striking thermal disparity. Temperatures range from 0 ° C to 62 ° C. Several hot points or surfaces are visible; Which proves that the different types of degradations identified previously decrease the electrical current. The cold parts identified represent the visual defects highlighted in the EL image. This photovoltaic module exposed for about ten (10) years shows a great thermal inhomogeneity, meaning an advanced electrical mismatch. This justifies the significant I_{SC} degradation and the decrease of the I_{MMP}

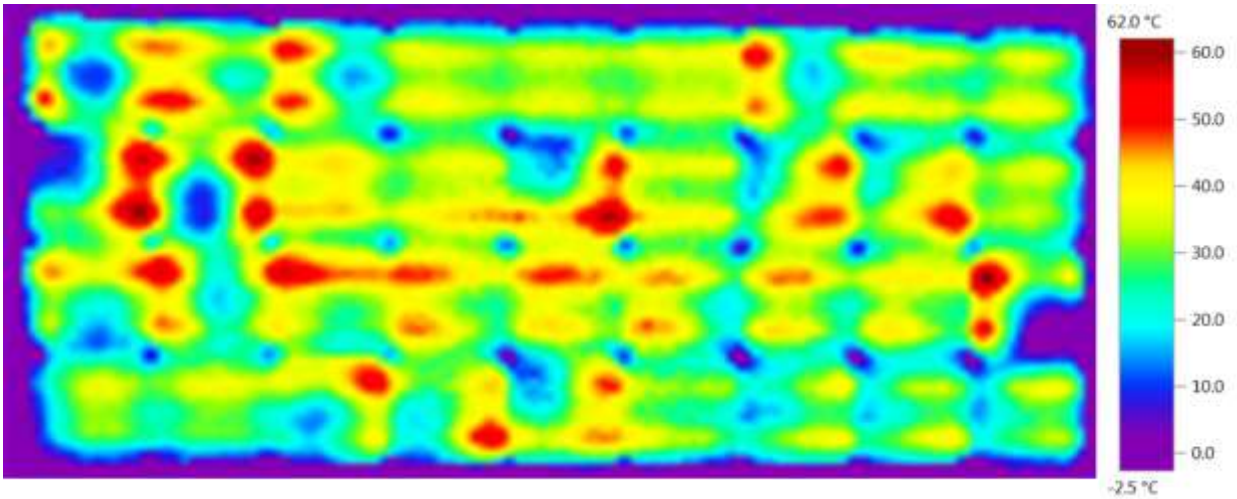

Figure 26: Module A IR Image

IV.3.2) Module B: Polycrystalline

IV.3.2.1) analysis by electroluminescence (EL)

IV.3.2.1.1) Degradation types identification

The EL image for polycrystalline module was realized under the same conditions as the previous analyzed monocrystalline. For defects identification, the EL image used is realized under the short circuit current (I_{SC})with different colors pointing fingers at the types of degradation present in the module (Figure **27**).

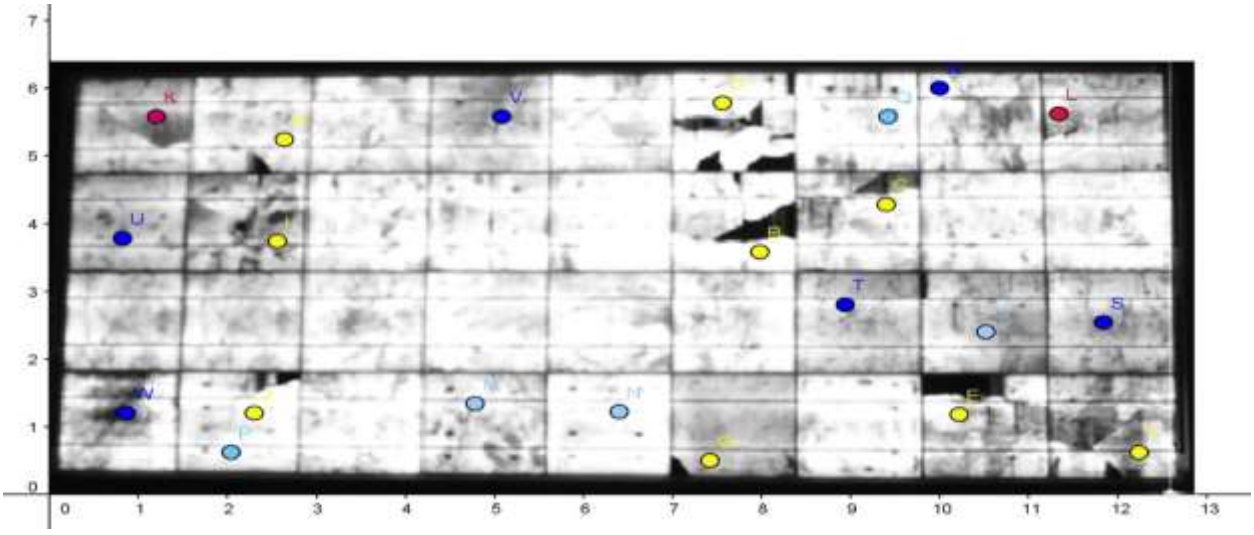

Figure 27: module B EL image with I= Isc

- **Nine (9) cells** of the polycrystalline module experienced fairly extensive breaks which isolated the broken cell parts.
- **Six (6) cells** have visual defects (**Figure 28**) due to the effects of the environment. During visual inspection, delamination of PV module's encapsulat has been identified. Which probably justifies the presence of these dark surfaces indicating visual degradation.

Figure 28: Module B Visual image

- **Five (5) cells** have localized shunts. This type of defects is generally due to problems during cell's manufacturing (a particle, an anomaly in growth, etc.). It may also be a consequence of an external event such as electrostatic discharge or mechanical stress.
- **Two (2) cells** have micro cracks which elongated the list of mechanical defects.

for the polycrystalline module, mechanical defects due to physical constraints are the most present defects. **Nine (9) cells** in total have breakages often very advanced, and 2 others have micro cracks.

Table 8: Defects observed in module B

Degradation type	Number of effected cells	Percentage relative to the total number of cell
micro cracks	2	5.56%
visual degradation	6	16.67%
localized shunt	5	13.89%
broken cells	9	25.00%

Concerning the material or visual defects often due to the effect of the environment, they are present on 6 cells which are not nevertheless very affected. Indeed, since a polycrystalline module is not homogeneous in nature, it is sometimes difficult to identify the photoelectric effect. Manufacturing defects also are still present with many localized shunts.

IV.3.2.1.2) Affected area Evaluation

Using the same software, and with the EL image of the polycrystalline at **I = 10%I_{SC}**, the results obtained show that the isolated surface is not very important. Seven (7) zones are isolated, representing a total area of 6.38 cm^2. So only 8.5% of the module's surface was severely affected, causing a degradation of -2.92% of the maximum power (P_{MPP}). Thus 3.5% of the power decreased to 1% of affected area.

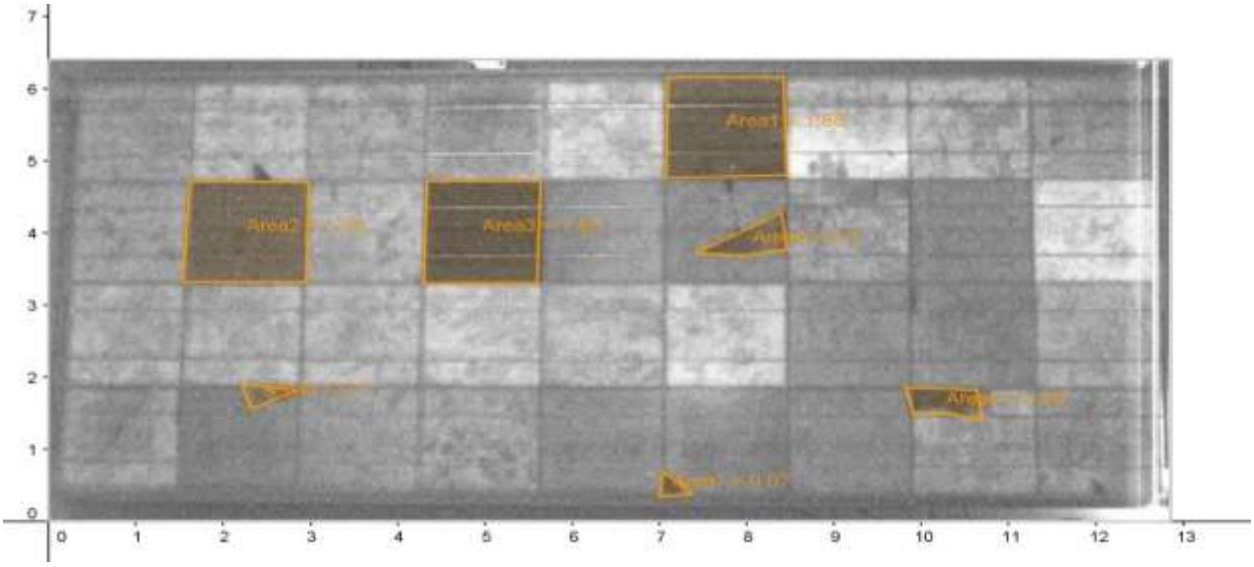

Figure 29: Module B EL image withe I= 10% Isc

However, it has always been pointed out that these isolated areas represent the consequences of all the

defects identified. Similarly, they are not totally eliminated from the module, even if their participation is weak they slightly participate in the functioning of the module.

IV.3.2.2) analysis by infrared imaging (IR)

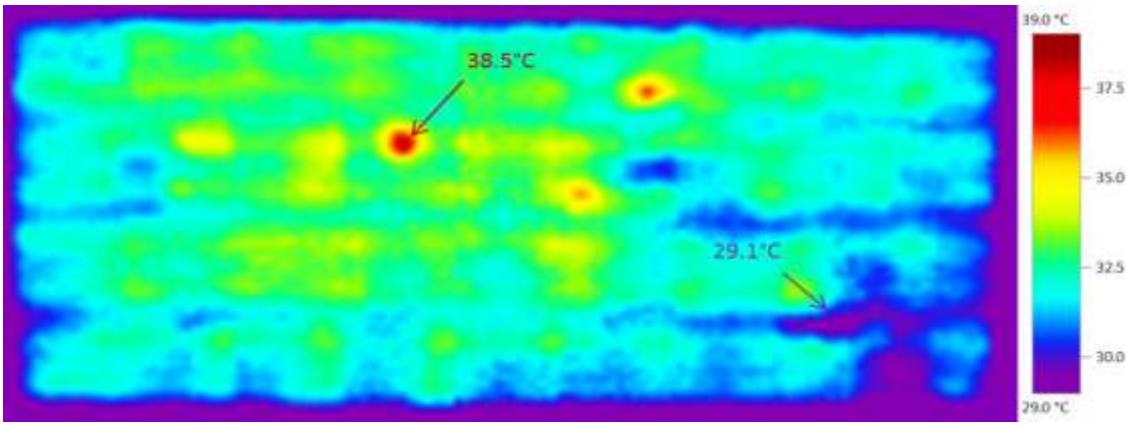

Figure 30: Module B IR image

The IR image of the polycrystalline module shows a more homogeneous thermal distribution compared to the mono. Temperatures range from 29 to about 39 ° C. The maximum temperature is not then so critical because it is less than the NOCT of 45°C. the biggest part of the surface has a temperature of about 30 ° C. Apart from 3 hot spots identified and some cold areas, the thermal disparity is not significant enough. Thus, the passage of the electric current is not too disturbed hence the low degradation of the current compared to the initial characteristics.

IV.4) Conclusion

The evaluation of the degradation already proves that the modules were affected after the years of exposure. The P_{MPP} degradation is equal to -5.35% for module A, and just -2.92% for module B. But it should be noted that the modules did not have the same degradation behavior. Module A experienced a significant drop in its short-circuit current (I_{SC}), while module B had a slight decrease in its nominal voltage V_{MPP}.

In this way, the visual inspection, EL and IR imaging allow to identify the different defects leading to such kind of degradation for the two modules. Even if there is not enough information on the degradation effects of each type of climate on the different crystalline technologies; defects due to the environmental conditions found in this study are much more present in the monocrystalline module than on the polycrystalline. The mechanical defects on the polycrystalline module are too advanced and will obviously be at the origin of most of the consequences on performance characteristics. The surface monocrystalline module isolated surface by the identified defects is much more important (27.96% of total area), compared to the poly (only 8.5% total area). finally, EL images of the two PV modules in this study show that with the technology used, the environmental effects have been much more felt on the single-crystalline one. However, the affected surface analysis shows that the effect of percentage of affected surface on the P_{MPP} are more important for the polycrystalline than the mono.

The IR image for the monocrystalline module well justifies extensive degradation of the short circuit current and maximum power. The Module Isc mismatch clear shown in the thermography with many hot spots means that those parts can no more produce the short circuit current. So, the damage previously identified as corrosion and discoloration decreased the electrical output of several cells. Indeed, in the IR image analysis with a current equal to I_{SC} shows a large rise in temperature which reached 60 ° C. This means that a big part of the module no longer produces enough power and transforms the surplus current coming from the healthy cells into heat. For the poly, the IR image shows that productivity is not too affected. The temperature distribution is almost homogeneous. We can then say that; the important mechanicals defects identified with the EL image do not affect too much the cells' production. Thus, by comparing the analyzes of the IR and EL images of the two modules it can be concluded that the defects caused by the climate on the mono module affect much more the production than the numerous mechanical defects on the poly.

CONCLUSIONS AND RECOMMENDATIONS

CONCLUSIONS AND RECOMMENDATIONS

The effects of exposition climate on performance degradation of photovoltaic modules operating under sub-Saharan environment in Senegal was studied in this Master thesis. Two different PV module technologies (mono & polycrystalline silicon) made by two different manufactures have been exposed during 10 years on the site of Ecole Supérieur Polytechnique, Dakar University in Senegal. PV modules' main electrical parameters (short-current, open voltage, maximum power, nominal current and voltage) are measured and translated to their correspondent STC values. The I-V curves obtained initially on operation site are compared to those measured about 10 years after. The absolute degradation for the module A is -5.35%, after ten years of exposure, the I_{SC} is the most affected characteristic for this module (-9.46%). However, absolute degradation for module B is very low, just -2.92% after 10 years of exposure.

This study shows from the visual inspection, the EL and IR images that Dakar's coastal climate has non negligible effects on the PV modules. The main degradation types found on the two modules are: encapsulant discoloration, delamination, breakage, oxidation, micro cracks, localized shunt, Contact finger interruption and non-identified dark areas after about 10 years of operation. The main degradations due to the climate (delamination, corrosion, discoloration, oxidation) are mostly found on the monocrystalline(A). The module B is less affected by such kind of degradation due to the climate. The other degradations that occur during manufacturing or installation are found on the two technologies. Apart from the contact fingers interruption on module A, the effects of the mechanical degradation were negligible. The defects from the environment are mainly due to the hot and humid climate influenced by the sea in this region.

The information from this master thesis about the degradation issues of the PV modules in this sub-Saharan area indicates that the monocrystalline silicon module is the most degraded technology. The defects also caused by the climate conditions are mainly found in this module. It may seem negligible losing about -6% in just one module after 10 years. But for like a PV 100 MW_P power plants made with this technology it will be a loss of

$6MW_P$ that could fuel an important number of households. And the small absolute degradation in the polycrystalline module and the very slight effects of the environment in this module leads to say that this technology is more suitable for this climate. This allows the designers of projects in this side of Africa to choose the best technology and take into account the losses due to the climatic environment when planning photovoltaic system.

In future works, we will explore the degradations and their causes in the other different climate zone of the country using the two different technologies as done in this work. This will allow to determine the suitable PV technology for all the climates and determine the expected degradation to take into account during designing.

References

[1] AIE, "African Energy Outlook : focus on Sub-saharan Africa countries," International Energy Agency, Paris, 2014.

[2] "The world Bank and Energy in Africa," World Bank, [Online]. Available: http://web.worldbank.org/WBSITE/EXTERNAL/COUNTRIES/AFRICAEXT/0,,contentMDK:21935594~pagePK:146736~piPK:146830~theSitePK:258644,00.html.

[3] G. Adolf, K. Joachim and B. Voss, Crystalline Silicon Solar Cells, Freiburg: John Wiley & Sons Ltd, 1998.

[4] 25 April 2009. [Online]. Available: https://www.aps.org/publications/apsnews/200904/physicshistory.cfm.

[5] H. M. Hubbard, "Photovoltaics Today and Tomorrow," *American Association for the Advancement of Science,* pp. 297-304, 1989.

[6] Ababacar Ndiaye. Etude de la degradation et de la fiabilite des modules photovoltaiques – Impact de la poussiere sur les caracteristiques electriques de performance. Sciences de l'ingenieur [physics]. Ecole Superieure Polytechnique (ESP) - UCAD, 2013. Français. <tel-01250271>

[7] Green MA. 2013 Silicon solar cells: state of the art. Phil Trans R Soc A 371: 20110413. http://dx.doi.org/10.1098/rsta.2011.0413.

[8] D. Sébastien, "Influence des interactions impureté-défaut et impureté-impureté sur le rendement deconversion des cellules photovoltaïques au silicium cristallin," UNIVERSITE PAUL CEZANNE AIX-MARSEILLE III, Marseille, 2007.

[9] P. Mohanty et al. (eds.), Solar Photovoltaic System Applications, Green Energy and Technology, Springer International Publishing Switzerland 2016 ,DOI 10.1007/978-3-319-14663-8_2

[10] I. Fraunhofer Institute for Solar Energy System, "PHOTOVOLTAICS REPORT," Fraunhofer ISE, 2016.

[11] N. SAHOUNE, "Chapitre 1: Etat de l'art des cellules solaires conventionnelles," Tlemcen, Université de Tlemcen, 2010.

[12] M. Hahn, "Solar cells," pv resources, 23rd December 2015. [Online]. Available: http://pvresources.com/en/solarcells/technologies.php. [Accessed 14 January 2017].

[13] M. Parimita, M. Tariq, J. G. Eulalia and K. Yash, "Solar Radiation Fundamentals and PV System Components," *Green Energy and Technology,* 2016.

[14] L. Denis, PVresources, 23rd December 2015. [Online]. Available: http://pvresources.com/en/solarcells/solarcells.php#notes. [Accessed 15th February 2017 at 18:16].

[15] L. Eduardo, Solar Electricity: Engineering of Photovoltaic System, Seville, (1994).

[16] F. Nicola, P. G. ,. Giovanni and V. Massimo, Power Electronics and Control Techniques for Maximum Energy Harvesting in Photovoltaic Systems, New York City: Taylor & Francis Group, 2013.

[17] H. S. Arno, J. Klaus, I. Olindo, A. v. S. René and Z. Miro, Solar energy: The physics and engineering of photovoltaic conversion, technologies and systems, Cambridge: 2016, 2016.

[18] H. Christiana and B. Stuart, "PV Education," [Online]. Available: http://www.pveducation.org/pvcdrom/fill-factor-0. [Accessed 22 February 2017].

[19] G. Michael, "Photovoltaic and photoelectrochemical conversion of solar energy," *Philosophical Transactions: Mathematical, Physical and Engineering Sciences,* pp. 993-1005, 2007.

[20] I. (2016), "REmap: Roadmap for a Renewable Energy Future," International Renewable Energy Agency (IRENA),, Abu Dhabi,, 21016.

[21] I. (2015), " Africa 2030:Roadmap for a Renewable Energy Future.," IRENA, Abu Dhabi., 2015.

[22] N. Ababacar, M. K. Cheikh, C. Abdérafi, A. N. Papa, S. Vincent and K. Abdessamad, "Degradation evaluation of crystalline-silicon photovoltaic modules after a few operation years in a tropical environment," *SOLAR ENERGY,* vol. 103, pp. 70-77, 2014.

[23] A. e. al, "Review of photovoltaic degradation rate methodologies," *Renewable and Sustainable Energy Reviews ,* vol. 40, p. 143–152, 2014.

[24] E. Kaplani, Renewable Energy in the Service of Mankind, vol. II, Switzerland: Springer International Publishing, 2016.

[25] J. Y. Ye, T. Reindl, A. G. Aberle and T. M. Walsh, "Singapore Performance Degradation of Various PV Module Technologies in Tropical," *IEEE JOURNAL OF PHOTOVOLTAICS,* vol. 4, pp. 1288-1294, 2014.

[26] Y. Hishikawa, K. Morita, S. Sakamoto and T. Oshiro, "FIELD TEST RESULTS ON THE STABILITY OF 2,400 PHOTOVOLTAIC MODULES MANUFACTURED IN 1990's," in *the Twenty-Ninth IEEE Photovoltaic Specialists Conference*, 2002.

[27] C. J. D and R. K. S, "PROGRESS IN PHOTOVOLTAICS: RESEARCH AND APPLICATIONS".*Photovoltaic Degradation Rates—an Analytical Review.*

[28] C. J. Dirk, H. W. John and R. K. Sarah, "Technology and Climate Trends in PV Module Degradation," in *27th European Photovoltaic Solar Energy Conference and Exhibition* , Frankfurt, Germany, 2012.

[29] IEA, "Review of Failures of Photovoltaic Modules," INTERNATIONAL ENERGY AGENCY, 2014.

[30] M. Munoz, M. Alonso-García, N. Vela and F. Chenlo, "Early degradation of silicon PV modules and guaranty conditions".

[31] Virtuani, A., Müllejans, H. and Dunlop, E. D. (2011), Comparison of indoor and outdoor performance measurements of recent commercially available solar modules. Prog. Photovolt: Res. Appl., 19: 11–20. doi:10.1002/pip.977

[32] S. Wendlandt, A. Drobisch, T. Buseth, S. Krauter and P. Grunow, "HOT SPOT RISK ANALYSIS ON SILICON CELL MODULES," in *25th European Photovoltaic Solar Energy Conference and Exhibition*, Valencia, 2010.

[33] F. D. S. Freire, "Performance and Degradation Analysis of Operating PV Systems," Rochester Institute of Technology, 2016.

[34] J.L.Crozier, E. Dyk and F.J.Vorster, "High Resolution Spatial Electroluminescence Imaging of Photovoltaic," Nelson Mandela Metropolitan University, Port Elizabeth, South Africa, 2009.

[35] E. Kaplani, "Degradation in Field-aged Crystalline Silicon Photovoltaic Modules and Diagnosis using Electroluminescence Imaging," in *8th International Workshop on Teaching in Photovoltaics*, Prague, 2016.

[36] A. Mansouri, M. Zett, O. Mayer, M. Lynass, M. Bucher, O. Stern, C. Heller and E. Mueggenburg, "Defect detection in photovoltaic modules using electroluminescence imaging," in *27th EU PVSEC –Defect detection in photovoltaic modules using electroluminescence imaging*.

[37] "Electroluminescence for PV Cells," SENSORS UNLIMITED, [Online]. Available: http://www.sensorsinc.com/applications/photovoltaics/electroluminescence-for-pv-cells. [Accessed 15 Jun 2017].

[38] P. Juraj, Milan, Perný, Š. Vladimír and M. Váry, "Chosen Diagnostic Methods of Photovoltaic Modules," in *IEEE Conference Publications*, 2016.

[39] Y. Hu, W. Cao, J. Ma, S. Finney and D. Li, "Identifying PV Module Mismatch Faults by a Thermography-Based Temperature Distribution Analysis," *IEEE,* 2013.

[40] J. A.Tsanakas, L. Ha and C. Buerhop, "Faults and infrared thermographic diagnosis in operating c-Si photovoltaic modules :A review of research and future challenges," *Renewable and Sustainable Energy Reviews,* 2016.

[41] M. Kontges, S. Kajari-Schroder and I. Kunze, "Crack Statistic for Wafer-Based Silicon Solar Cell Modules in the Field Measured by UV Fluorescence," *IEEE JOURNAL OF PHOTOVOLTAICS,* vol. 3, 2013.

[42] R. Beate, S. Jan and K. Michael, "FLUORESCENCE IMAGING FOR ANALYSIS OF THE DEGRADATION OF PV MODULES," *IEEE JOURNAL OF PHOTOVOLTAICS,* vol. 3, 2013.

[43] [Online]. Available: https://www.infoclimat.fr/climatologie/annee/2016/dakar-yoff/valeurs/61641.html.

[44] [Online]. Available: https://fr.climate-data.org/location/518111/.